$PM_{2.5}$ chemical composition and health risks by inhalation near a chemical complex

Célia Alves[1*], Margarita Evtyugina[1], Estela Vicente[1], Ana Vicente[1], Ismael Casotti Rienda[1], Ana Sánchez de la Campa[2,3], Mário Tomé[4], Iola F. Duarte[5]

[1]*Department of Environment, Centre for Environmental and Marine Studies (CESAM), University of Aveiro, 3810-193 Aveiro, Portugal*

[2]*Associate Unit CSIC-University of Huelva "Atmospheric Pollution", Centre for Research in Sustainable Chemistry - CIQSO, University of Huelva, E21071 Huelva, Spain*

[3]*Department of Mining, Mechanic, Energetic and Construction Engineering, ETSI, University of Huelva, 21071 Huelva, Spain*

[4]*PROMETHEUS, School of Technology and Management (ESTG), Polytechnic Institute of Viana do Castelo, 4900-348 Viana do Castelo, Portugal*

[5]*Department of Chemistry, CICECO - Aveiro Institute of Materials, University of Aveiro, 3810-193 Aveiro, Portugal*

ABSTRACT

With the aim of performing a detailed characterisation of the organic and inorganic constituents of particulate matter ($PM_{2.5}$), as well as an estimate of the risks of exposure through inhalation, a monitoring campaign was carried out, for the first time, in the vicinity of the industrial chemical pole of Estarreja, one of the largest in Portugal. Daily $PM_{2.5}$ samples were analysed for organic and elemental carbon (OC and EC), 47 trace elements and around 150 organic constituents. On average, OC and EC accounted for 25.2% and 11.4% of the $PM_{2.5}$ mass, respectively. Organic compounds comprised polycyclic aromatic hydrocarbons (PAHs), alkylated PAHs, anhydrosugars, phenolics, aromatic ketones, glycerol derivatives, aliphatic alcohols, sterols, and carboxyl groups, including aromatic, carboxylic and dicarboxylic acids. Enrichment factors > 100 were obtained for Pb, Cd, Zn, Cu, Sn, B, Se, Bi, Sb and Mo, showing the contribution of industrial emissions and nearby major roads. Principal component analysis revealed that vehicle, industrial and biomass burning emissions accounted for 66%, 11% and 9%, respectively, of the total $PM_{2.5}$-bound PAHs. Some of the detected organic constituents are likely associated with plasticiser ingredients and thermal stabilisers used in the manufacture of PVC and other plastics in the industrial complex. Photooxidation products of both anthropogenic (e.g., toluene) and biogenic (e.g., isoprene and pinenes) precursors were also observed. It was estimated that biomass burning accounted for 13.8% of the $PM_{2.5}$ concentrations and that secondary OC represented 37.6% of the total OC. The lifetime cancer risk from inhalation exposure to $PM_{2.5}$-bound PAHs was found to be negligible, but it exceeded the threshold of 10^{-6} for metal(loi)s, mainly due to Cr and As.

* Corresponding author. E-mail: celia.alves@ua.pt

Keywords: $PM_{2.5}$, OC/EC, organic speciation, trace elements, cancer and non-cancer risks

Introduction

Air pollution leads to premature deaths from heart disease, stroke, and cancer, as well as acute lower respiratory infections (Bowe et al., 2019; Sharma et al., 2020; Yin et al., 2020). According to data from the World Health Organisation (WHO), it is estimated that indoor and outdoor (ambient) air pollution causes every year 7 million deaths globally (WHO, 2016). It is the 4th leading risk factor for mortality worldwide, ahead of other well-known risks like alcohol use and physical inactivity (HEI, 2020). In Europe, air pollution is the single largest environmental health risk and a major cause of premature deaths and diseases (EEA, 2020). The International Agency for Research on Cancer has classified air pollution in general, and specifically particulate matter lower than 10 and 2.5 μm (PM_{10} and $PM_{2.5}$), as carcinogenic. Particulate matter was recognised as the deadliest form of air pollution (IARC, 2013). As a result of exposure to $PM_{2.5}$, about 400,000 premature deaths per year occur in the 39 member countries of the European Environmental Agency (EEA, 2020), excluding Turkey. Based on the WHO's Global Burden of Disease Project (GBD 2019 Risk Factors Collaborators, 2020), $PM_{2.5}$ was pointed out as one of the main responsible for the largest increases in risk exposure. Particulate matter pollution burden was 44.6% higher in GBD 2019 than in GBD 2017. The rise is mainly due to the inclusion of low birthweight and short gestation as risk factors that are themselves affected by $PM_{2.5}$, as well as increases in the relative risk curve for cardiovascular diseases.

The toxicity, and consequently the health effects, of $PM_{2.5}$ is highly dependent on its chemical composition (Park et al., 2018). So far, most of the works carried out in urban and industrial areas have mainly focused on polycyclic aromatic hydrocarbons (PAHs), due to their known carcinogenicity (e.g., Alves et al., 2017; Chao et al., 2019; Elzein et al., 2020; Fang et al., 2020, Hu et al., 2017; Liu et al., 2019; Wang et al., 2015, 2016; Wu et al., 2014; Yan et al., 2017; Zhang et al., 2019; Zhu et al., 2019). However, some studies have recently outlined the role of multiple chemical components, such as polar organics, in inducing cytotoxicity, genotoxicicity or DNA damage (Besis et al., 2017; Jia et al., 2017; Van Den Heuvel et al., 2018). Particulate matter mass concentrations alone are not able to explain the health outcomes. Therefore, further research is essential to better understand the chemical specificities of the particulate material.

The town of Estarreja is an interesting area for air quality studies, given the proximity to one of the most important industrial areas in Portugal and to some major roadways. The heavy industry is mainly located inside the so-called "Estarreja Chemical Complex". This industrial area of 2 km^2 is 1 km away from the town. The most significant industrial units, working for many decades, are dedicated to the production of: i) nitric acid, aniline and nitrobenzene, ii) sodium and chlorate compounds from rock salt through electrolytic cells, iii) synthetic resins, mainly PVC (polyvinyl chloride) from vinyl chloride monomer (VCM), and iv) isocyanide polymers of aromatic base. In 2009, the industrial pole was

expanded and the so-called "eco-business park" was created, integrating nowadays about 30 companies, spread over an area of 290 ha. This park accommodates different economic activities, including industrial, commercial, warehousing and services. According to the annual air quality reports of the Portuguese Environment Agency, the $PM_{2.5}$ yearly mean values in Estarreja have been close to or exceeded the WHO guideline (10 $\mu g/m^3$), although remaining within acceptable values set by national/European legislation (< 25 $\mu g/m^3$). A deeper understanding of the impacts of $PM_{2.5}$ on human health is crucial to support policy making and public awareness on air pollution. A previous air quality assessment, involving data from 2000 to 2009, was carried in Estarreja, but only traditional pollutants from the local station (SO_2, NO_x, O_3 and PM_{10}) were considered (Figueiredo et al., 2013). Despite being based on a short-term sampling campaign, the present work is the first carried out in Estarreja covering a detailed characterisation of both the organic and inorganic constituents of $PM_{2.5}$, as well as an estimate of the risks associated with inhalation exposure. Thus, it is expected that this preliminary work can contribute to a better understanding of the sources and causes of the possible adverse effects, not only in Estarreja, but also in other regions impacted by emissions from the chemical industry as well.

Methodologies

Sampling

Sampling took place in the municipality of Estarreja, with about 30,000 inhabitants, from September 20th to November 9th, 2019. The city itself has a population of approximately 7,000. The municipality has developed along the banks of the Antuã river, near the Aveiro lagoon, which is located on the Atlantic coast of central Portugal, covering an area of about 75 km^2. In parallel with its important industrial pole, Estarreja has always been a region with both intensive and extensive farming. The municipality is crossed by relevant roadways, such as two motorways that connect Lisbon-Porto and by a national road that connects other cities in the central region to Porto.

Three low volume samplers (TCR Tecora, model 2.004.01), equipped with $PM_{2.5}$ inlets and operating at a flow of 2.3 m^3/h, were installed on the rooftop of one of the building of the secondary school of Estarreja (lat.: 40.758553; long.: -8.567158), which is approximately 1 km from the industrial complex (Fig. S1). One of the instruments was equipped with quartz fibre filters, while the other two were deployed with Teflon filters, all from Pall Corporation. Three samples were taken in parallel for 24 h, every 2 days, starting at 00:01 and ending at 23:59 (local time). A portable meteorological station (Davis Instruments) was also installed on the roof. Temperature, relative humidity, wind direction and speed were continuously measured using a Vantage Pro 2 console with the Integrated Sensor Suite (ISS) program and the WeatherLink software for data processing. An air quality station, classified as suburban, is located at the school. It belongs to the monitoring network of the Portuguese Environmental Agency, and provides hourly data of PM_{10}, $PM_{2.5}$, O_3 and NO_x.

Analytical techniques

$PM_{2.5}$ filters were weighted in an analytical microbalance with 1 μg readability (Radwag 5/2Y/F). Gravimetric concentrations for each sample were obtained from the average of six measurements in a temperature and humidity-controlled room (20 ºC and 50%). A portion of each quartz filter was used for the determination of the organic (OC) and elemental carbon (EC) by a thermal optical transmission technique, according to the protocol already described in previous publications (Alves et al., 2011; Pio et al., 2011). The remaining area of each quartz filter was digested with a mixture of acids (2.5 mL HNO_3: 5 mL HF: 2.5 mL $HClO_4$), following the methodology proposed by Querol et al. (2001) for the quantification of elements by inductively coupled plasma atomic mass spectrometry (ICP-MS, Agilent 7900). The analytical error was estimated by repeated analysis of a certified reference material (NBS-1633b, fly ash). An accuracy of 5-10% was estimated. For each pair of Teflon filters, one was dedicated to the determination of nonpolar organic compounds, while the other was subjected to the analysis of polar constituents. Polar organic compounds were extracted by ultrasonication for 10 min using 25 mL of ethyl acetate/hexane. After a 5 min rest, the filter was extracted 2 times with 25 mL of formic acid (4%) and methanol, with a 5 min stop between extractions. Nonpolar compounds were also extracted by ultrasonication using a mixture of hexane and toluene (3 consecutive extractions with 25 mL for 10 min each, with 5 min stops between them). The final 75 mL volumes of either the polar or nonpolar fractions were concentrated to 0.5 mL using a Turbo Vap® II evaporation system (Biotage). The extracts were then dried under a gentle nitrogen stream. Nonpolar compounds were analysed in a gas chromatographer-mass spectrometer (GC-MS) from Shimadzu (model QP5050A) equipped with a TRB-5MS 30 m × 0.25 mm × 0.25 μm column (Vicente et al., 2019). Polar compounds were converted to trimethylsilyl derivatives and quantified in a GC-MS from Thermo Scientific (TRACE GC Ultra) with a DSQ II detector and equipped with a TRB-5MS 60 m × 0.25 mm × 0.25 μm column, following the chromatographic conditions described in Alves et al. (2011). Blank filters were treated in the same way as the samples and their concentrations subtracted from those of $PM_{2.5}$.

Air mass backward trajectories and data analysis

Backward air mass trajectories were calculated at 00:00, 06:00, 12:00 and 18:00 UTC, with a run time of 72 h and an arrival height of 100 m above ground level using the HYSPLIT (HYbrid Single-Particle Lagrangian Integrated Trajectory) model (Draxler and Rolph, 2015), developed by the U.S. National Oceanic and Atmospheric Administration (NOAA). The model was run with the National Centre for Environmental Prediction's (NCEP) Global Data Assimilation System (GDAS, 1°) dataset.

The Openair package, which is available within the statistical software environment R, was used for plotting pollution roses. Principal component analysis (PCA), correlations and statistical significance levels were obtained through the SPSS software (IBM Statistics software v. 24).

Inhalation risk assessment

One of the most common exposure assessment methods that has been used in epidemiology considers that ambient levels are representative of the total population exposure, given the lack of time-activity patterns for distinct microenvironments (Kazakos et al., 2020). Thus, outdoor levels are generally taken as a surrogate of daily 24 h exposure. Following the methodology proposed by the United States Environmental Protection Agency (USEPA), and described in Alves et al. (2020), noncarcinogenic and carcinogenic risks resulting from inhalation of $PM_{2.5}$-bound elements and polycyclic aromatic hydrocarbons (PAH) were estimated. Target hazard quotients (THQ) and target carcinogenic risks (TR) associated with exposure to elements were calculated as follows:

$$THQ = (EF \times ED \times ET \times C)/(R_fC \times AT) \quad (1)$$

$$TR = (EF \times ED \times ET \times C \times IUR)/AT \quad (2)$$

where THQ and TR are dimensionless, EF is the exposure frequency (365 days per year), ED is the exposure duration (70 years), ET is the exposure time (24 h/day), C is the metal(loid) concentration (mg m^{-3}), and AT is the averaging time (70 years, i.e. 613,200 h). R_fC represents the reference concentration (mg m^{-3}) tabulated by USEPA (2017, 2019). For elements that have not yet defined an R_fC, values were derived from reference doses for oral exposure (R_fD, mg/kg/day), as suggested by USEPA (2013):

$$R_fC = (R_fD \times BW) / IR \quad (3)$$

where IR is the average inhalation rate for an adult (20 m^3/day) and BW is the body weight (70 kg). The chronic inhalation unit risk (IUR) values for the carcinogenic elements were taken from USEPA (2017). A THQ <1 indicates no significant or acceptable risk, a THQ > 1 suggests that noncarcinogenic effects are expected to happen, and a THQ > 10 reveals a high chronic risk. A TR < 10^{-6} suggests that exposure by inhalation of carcinogenic metals contributes to negligible risks, but caution is recommended to guarantee that the cumulative cancer risk for all potential cancer inducers does not surpass 10^{-4}.

The carcinogenic risk of a PAH mixture is frequently represented by its benzo[a]pyrene equivalent concentration (BaP_{eq}), which is calculated by multiplying the levels of individual compounds (PAH_i) by the respective toxicity equivalent factor (TEF_i) (Nisbet and NaGoy, 1992). The lifetime lung cancer risk is estimated through eq. (2), where C is ΣBaP_{eq}, and IUR is the inhalation unit risk of respiratory

cancer for BaP_{eq} (1.1×10^{-6} m^3/ng). The lifetime cancer risks are classified as very low when values are $\leq10^{-6}$.

Results and Discussion

Air quality

During the sampling campaign, the maximum hourly concentration of NO_2 (24.0 µg/m^3) and maximum daily mean (12.8 µg/m^3) did not surpass, respectively, the 1-h and 24-h standards of 200 µg/m^3 and 50 µg/m^3 imposed by the European Air Quality Directive (2008/50/EU). The maximum daily 8-h means of O_3 ranged from 26.8 to 67.3 µg/m^3, never exceeding the threshold of 120 µg/m^3.

Good correlations were observed between the gravimetric concentrations of the 3 samplers, presenting Pearson coefficients (r) of 0.913-0.987 ($p < 0.001$), slopes around 1 and intercepts close to 0. Correlations between gravimetric concentrations and values from the beta attenuation monitor of the air quality station were also statistically significant ($r = 0.956$-0.963, $p < 0.001$). On average, the levels measured at the air quality station represented approximately 80% of the concentrations obtained by the gravimetric reference method. The $PM_{2.5}/PM_{10}$ ratio obtained from real time measurements was 0.45±0.12. Daily PM_{10} concentrations were always below the threshold of 50 µg/m^3 imposed by the air quality directive. The daily values of $PM_{2.5}$ obtained gravimetrically ranged between 5.71 and 26.4 µg/m^3. The guideline value of 25 µg/m^3 recommended by WHO ($PM_{2.5}$ 24-h mean) was very slightly exceeded in two days of the sampling campaign.

North-western, western and south-western Atlantic advections accounted for 24%, 36% and 11% of the air mass trajectories arriving at Estarreja (Fig. 1). The highest $PM_{2.5}$ concentrations were associated with north Atlantic air masses, which, upon entering Portugal through the Leiria district, shifted their direction. On the way to the sampling site, these air masses crossed densely populated areas.

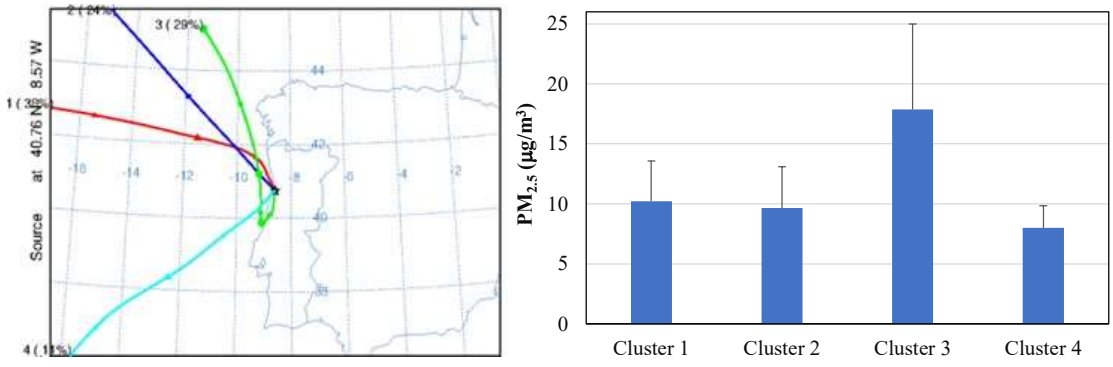

Fig. 1. Clusters of air mass backward trajectories and associated $PM_{2.5}$ concentrations.

The annual limit values for the protection of human health set by the European Union Directive 2004/107/EC for arsenic, cadmium and nickel (6, 5, and 20 ng/m^3 for As, Cd, and Ni, respectively) and by the Directive 2008/50/EC for lead (500 ng/m^3) in ambient air were not exceeded.

Carbonaceous and elemental composition of $PM_{2.5}$

OC and EC represented 25.2±14.6% and 11.4±7.2% of the $PM_{2.5}$ mass, respectively. A strong and significant correlation was found between OC and EC ($r = 0.941$, $p < 0.001$), indicating common sources, such as road traffic and biomass burning. The OC/EC minimum ratio method was used to estimate the secondary organic carbon (SOC) content (Pio et al., 2011). It was observed that SOC accounted for 37.6±17.5% of total OC. Thus, on average, about 10% of the $PM_{2.5}$ was composed of SOC. If a multiplying factor of 2 is taken to convert organic carbon into organic matter (Gao et al., 2015; Xie et al., 2013), this means that around 20% of the aerosol mass was photochemically produced. In Xiamen, a port city on the south-eastern coastal line of China suffering from rapid urbanisation and industrialisation, the carbonaceous aerosol represented 42.8-47.3% of the $PM_{2.5}$ mass. On average, SOC accounted for approximately 56% of OC (Zhang et al., 2011). Benetello et al. (2017) collected daily $PM_{2.5}$ samples in a large industrial area (Porto Marghera, Venice, Italy) during a 1-year-long sampling campaign. OC constituted 28% and 14% of $PM_{2.5}$ during the cold and warm periods, respectively, while the contributions of EC, for the same seasons, were 7.8% and around 9%.

In the present study, 47 elements were quantified in the $PM_{2.5}$ samples (Table 1) with total concentrations ranging from 24.2 to 133 ng/m^3. Altogether these elements constituted 0.230 - 1.26% of the $PM_{2.5}$ mass.

Table 1. Concentrations (ng/m^3) of trace elements detected in $PM_{2.5}$.

	Minimum	Maximum	Average
Li	<0.01	0.701	0.137
B	<0.01	28.1	8.12
Sc	nd	0.0753	<0.01
V	<0.01	8.89	2.13
Cr	<0.01	5.74	0.800
Co	<0.01	0.0830	0.0193
Ni	<0.01	2.11	0.534
Cu	1.06	15.3	4.66
Zn	4.11	44.5	21.2
Ga	<0.01	0.110	0.0205
Ge	nd	0.091	<0.01
As	<0.01	0.609	0.105
Se	<0.01	0.148	0.0586
Rb	<0.01	1.04	0.421

Sr	0.115	1.41	0.538
Y	<0.01	0.0706	0.0136
Zr	<0.01	2.46	0.447
Nb	nd	0.0665	<0.01
Mo	<0.01	51.1	17.3
Cd	<0.01	0.321	0.0604
Sn	0.0357	5.37	2.24
Sb	0.0318	6.25	0.845
Ba	0.289	5.10	2.40
ΣREE	nd	1.46	0.181
Hf	nd	0.0100	<0.01
W	<0.01	0.924	0.109
Pb	0.320	9.07	3.78
Bi	<0.01	0.733	0.175
Th	nd	0.0388	<0.01
U	nd	0.0120	<0.01

<0.01: below detection limit. Elements always below the detection limit for all samples: Be, Cs, Eu, Tb, Ho, Tm, Yb, Lu, Ta, Tl. nd – not detected. ∑REE: sum of Rare Earth Elements (from La to Er).

Among them, Zn, Mo and B were the most abundant. The chemical industrial complex of Estarreja includes a plastic (mainly PVC) manufacturing plant. Furthermore, the adjacent eco- business park also integrates various plastic and rubber product manufacturing companies. Thermal stabilisers, lubricant, and plasticisers are three crucial additives for processing PVC. Common thermal stabilisers of PVC include lead salts, organotin, rare earth, calcium and zinc soap salts (especially calcium and zinc stearates). Calcium stearate ($CaSt_2$) and zinc stearate ($ZnSt_2$) stabilisers are widely used since they have good lubricating properties and are relatively easy to process (Han et al., 2019). Besides, Zn is also related to traffic emissions (exhaust and non-exhaust). Zinc can be released from the engine exhaust deriving from the fuel, friction and wear of engine components, and lubricant oil additives (Agarwal et al., 2018). Additionally, the presence of zinc in particles resulting from brake and tyre wear is well documented (Penkała et al., 2018; Piscitello et al., 2021). The dual origin is proven by the pollution rose (Fig. 2), in which higher Zn concentrations can be seen when winds with higher speeds blow from the 4th quadrant, where the industrial complex is located, but also from other quadrants that cover the extensive road network of Estarreja.

Molybdenum sources include brake wear since molybdenum trioxide is used to prevent thermal fade and cracking of friction lining under high-temperature conditions (Adamiec, 2017; Valotto et al., 2015). This element is also used as an additive to improve the lubricant oil properties and to prevent oxidation and corrosion (Valotto et al., 2015). Mo is also used in the preparation of ceramic glazes and in the manufacture of steel alloys. The highest levels were recorded for winds from the W-N sector, suggesting an origin mostly in the industrial complex. Boron is mainly employed by the glass-ceramic industry. Additionally, this element is also used in the production of detergents, metal alloys, fire retardants, and

chemical fertilisers (Kot, 2009). The highest boron concentrations were observed in samples impacted by winds from the 4th quadrant, as well as from the NW direction. It should be borne in mind that Estarreja is surrounded by agricultural areas. In addition, the industrial park integrates a manufacturing unit dedicated to the production of metal parts for various sectors, whose capabilities comprise stamping, welding, as well as tube bending and forming. Factories producing home appliances (e.g., freezers and refrigerators) and equipment for clinical, rehabilitation and geriatric health (e.g., beds and cabinets), and a unit dedicated to the manufacture of fine stoneware products are also based in the eco-business park and may contribute to the emission of metal(loi)s.

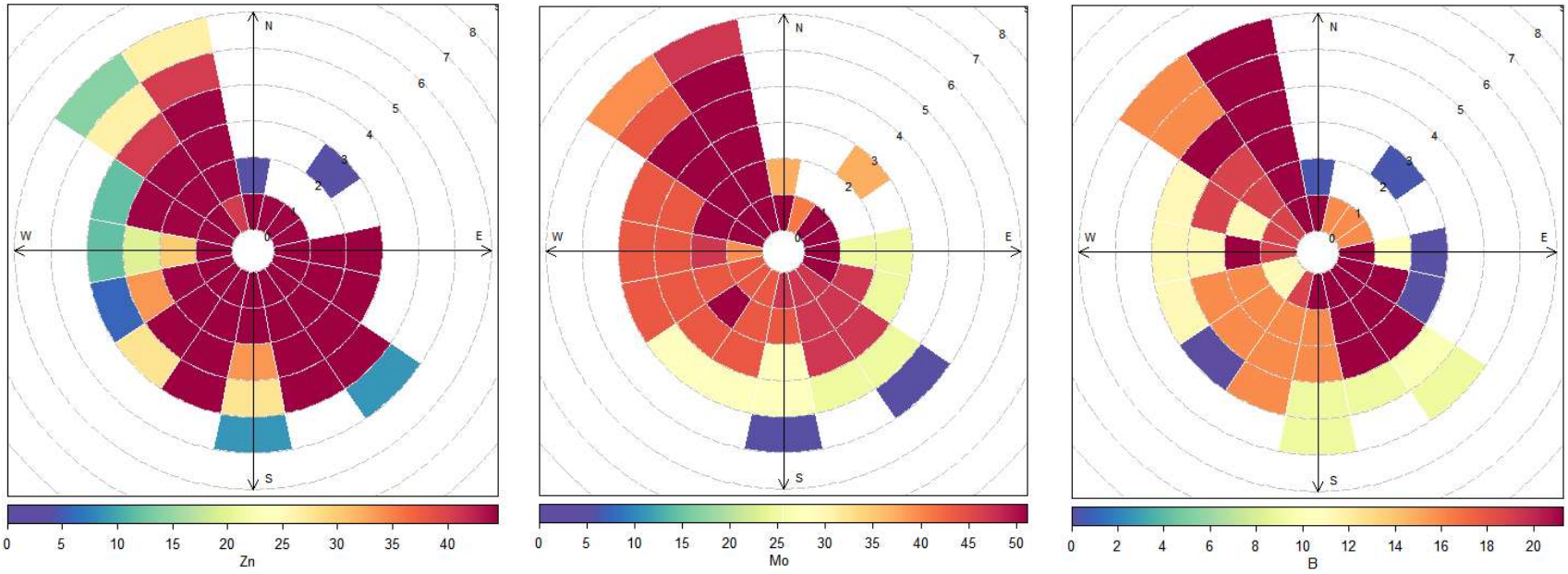

Fig. 2. Pollution roses for the most abundant metals. Wind speeds and concentrations are given in m/s and ng/m^3, respectively.

To identify the input of anthropogenic sources to the levels of a specific element in airborne particles, enrichment factors (EF) were determined (Fig. 3). Lithium was used as reference element since it is an abundant element of the Earth's upper continental crust (Moreno et al., 2006). The calculations were based on the average chemical composition of the upper continental crust given by Wedepohl (1995), according to the following equation:

$$EF = (CE_i/C_{Li})_{air}/(CE_i/C_{Li})_{crust} \quad (4)$$

where CE_i represents the concentrations of the element under analysis and C_{Li} is the concentration of lithium in the air or in the crust as indicated in the subscript. Enrichment factors above 10 indicate that the element arises mainly from anthropogenic sources while for lower EFs the element is considered to have mostly a mineral origin (crustal) (Acciai et al., 2017; Zhang et al., 2018).

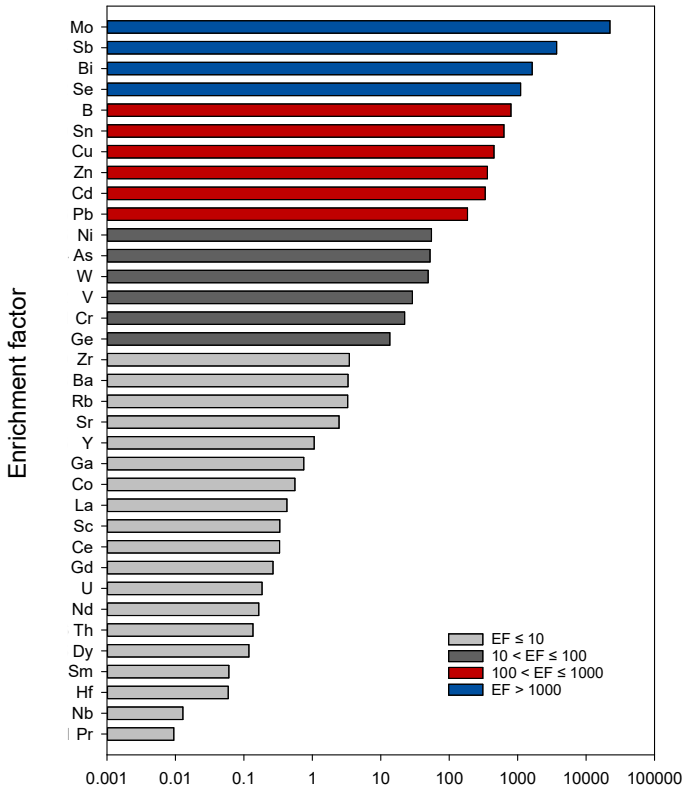

Fig. 3. Average enrichment factors of selected elements in $PM_{2.5}$.

Moderate EFs ($10 < EF \leq 100$) were recorded for Ge, Cr, V, W, As and Ni. Nickel and V are two elements that in association are generally linked to fuel oil combustion; however, no significant correlations were found between these two constituents in the present study. The main anthropogenic sources of arsenic are mining, use of pesticides and coal combustion (González et al., 2021). In the city of Huelva, Querol et al. (2004) found high levels of As and Cu and ascribed these two elements to the

metallurgical industry. In the present study, significant positive correlations were found between these two elements ($r = 0.606$, $p = 0.003$) pointing to a similar source. Average EFs between 100 and 1000 were observed for Pb, Cd, Zn, Cu, Sn and B. Cadmium was used for a long time as stabiliser in PVC. However, with the restrictions on the use of Cd compounds in plastics, it started to be used mainly in decorative pigments in the ceramic industry (Turner, 2019). Similarly to Zn, other elements such as Pb, Cd, Cu and Sn have been related to non-exhaust emissions from traffic (Grigoratos and Martini, 2015; Penkała et al., 2018; Piscitello et al., 2021). In the present study, significant correlations were found between Zn and Pb ($r = 0.601$, $p = 0.003$) and Zn and Cd ($r = 0.443$, $p = 0.039$), suggesting common sources. Additionally, Zn was also found to be significantly correlated with Ba ($r = 0.580$, $p = 0.005$). Barium has been used as tracer for brake wear since it is used as filler, in the form of $BaSO_4$, to reduce manufacturing costs and to improve manufacturability of the brake lining (Grigoratos and Martini, 2015; Valotto et al., 2015). Higher EFs (> 1000) were found for Se, Bi, Sb and Mo. With regard to Bi, this element is mainly associated with refuse incineration, fossil fuel combustion, ferromanganese alloys and aluminium production (Ferrari et al., 2000). Additionally, it is worthwhile to note that bismuth molybdate catalysts are employed in the manufacture of acrylonitrile by the selective oxidation of propylene with ammonia (Brazdil, 2017; Ojebuoboh, 1992). Antimony is used in the manufacture of brake linings (Sb_2S_3) to reduce vibration and improve friction stability, and for that reason it is commonly used as tracer for brake wear (Valotto et al., 2015). Significant correlations were found between Sb and Cu ($r = 0.756$, $p < 0.001$) and between Sb and As ($r = 0.758$, $p < 0.001$). In previous studies, levels of Sb in association with Cu have been linked to brake abrasion from road traffic (Querol et al., 2007). The EFs obtained for the remaining elements were below 10, suggesting a crustal origin.

Polycyclic aromatic hydrocarbons

Total concentrations of PAHs ranged from 0.051 to 15.2 ng/m^3, averaging 4.69 ng/m^3. Phenanthrene, anthracene, fluoranthene and pyrene were absent from the samples. In general, the most abundant PAH was benzo[e]pyrene (Fig. 4). It occurs as a result of incomplete combustion and is found in coal, oil, gas, automobile exhaust, grilling emissions and biomass burning smoke. Some alkylated PAHs were also detected: C1 to C3-naphthalenes, C1- and C2-fluorenes, C1- and C3-fluoranthenes, C1-pyrenes, C1-chrysenes, and C3- and C4-dibenzothiophenes. It has been described that these compounds are more persistent and often more toxic than the non-alkylated PAHs, the toxicity increases with the number of alkyl substitutions on the aromatic ring, and diesel/biodiesel makes a significant contribution to their formation (Casal et al., 2014). The total mean concentration of alkylated PAHs was 0.809 ng/m^3, ranging from 0.071 to 2.13 ng/m^3.

Following the detailed descriptions provided by Xie et al. (2013) and Gao et al. (2015), the concentrations of PAHs in the gas phase were estimated by the gas/particle partitioning theory (Pankow, 1994a,b). The calculation was only possible for those compounds for which vapour pressures and

enthalpies of vaporisation are tabulated in the literature. It was observed that the 2-3 ring PAHs were almost totally in the gas phase, the 4 ring compounds were partitioned between the gas phase (54%) and the particulate phase (46%), while the heavier congeners were mostly in the condensed form (Fig. 5).

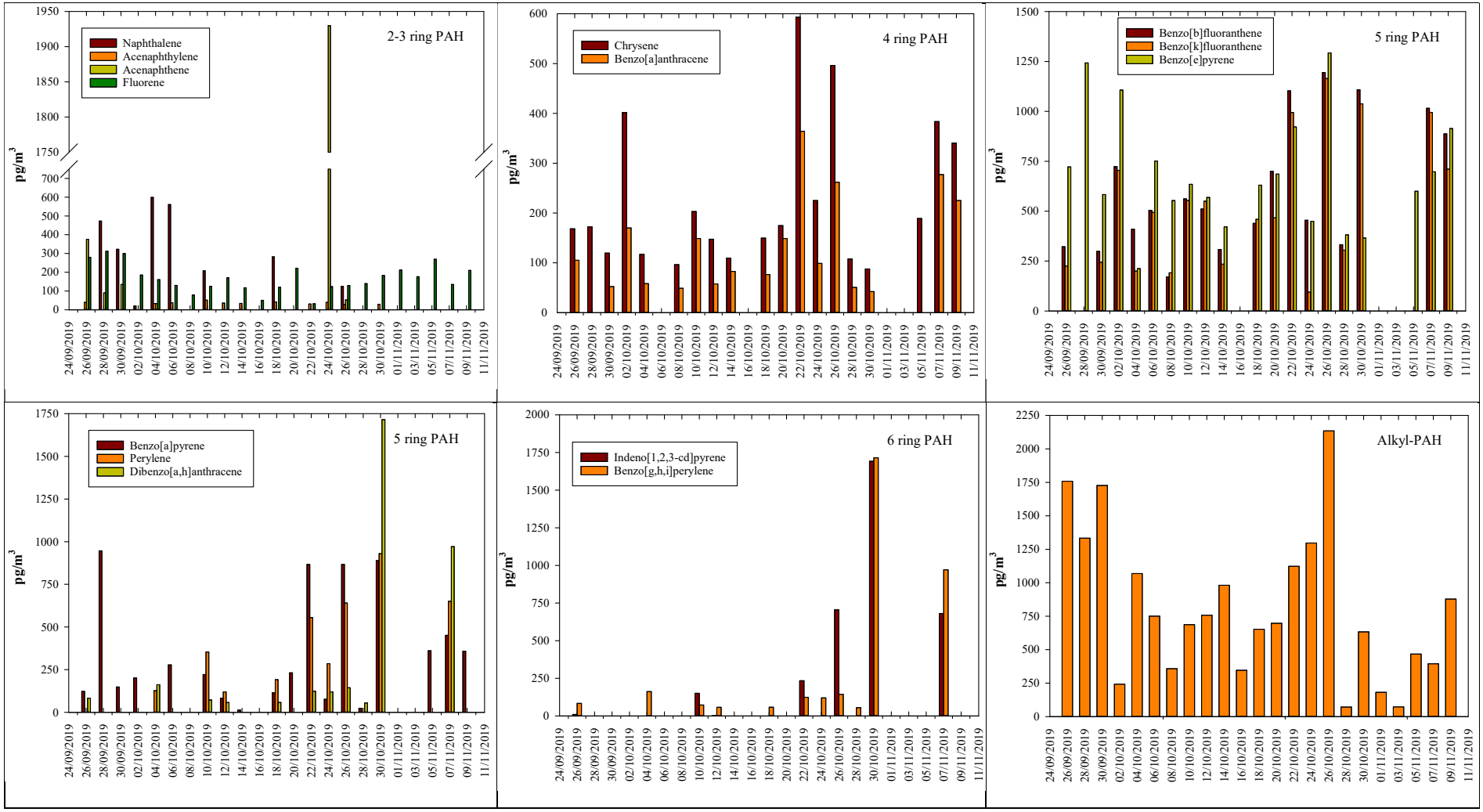

Fig. 4. Concentrations of PAHs in the particulate phase.

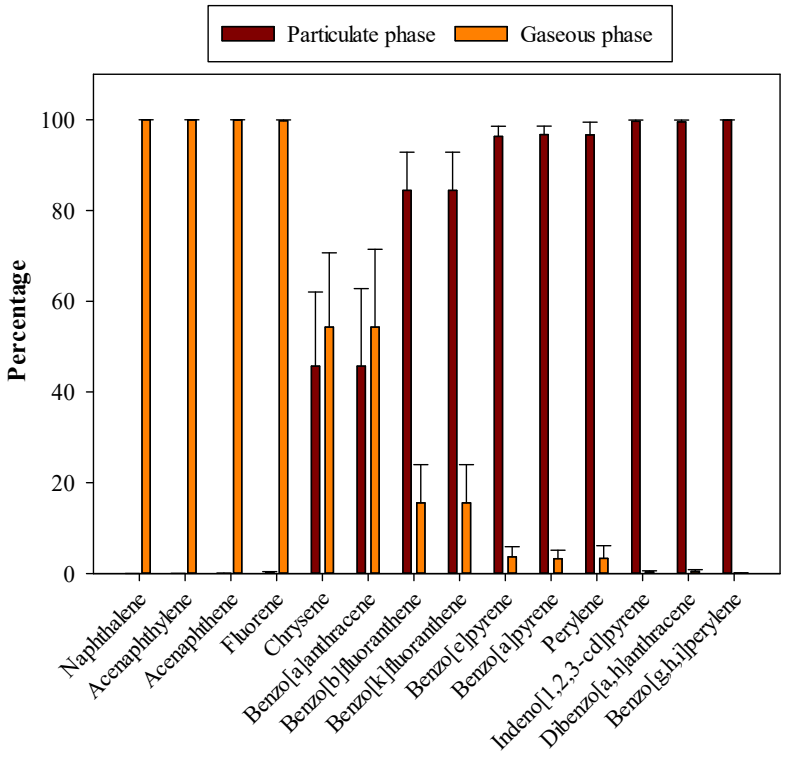

Fig. 5. Partition of PAHs between the gas and particle phases.

To identify the main sources of $PM_{2.5}$-bound PAHs, principal component analysis was carried out (Table 2). The PAH profile was determined by normalising the individual levels by the total PAH concentrations. Factor 1, which accounted for 66.1% of the total variance, was associated with high loadings on heavier PAHs emitted by gasoline exhausts, such as benzo[g,h,i]perylene, but also on lower molecular weight members (e.g., fluorene and benzo[b+k]fluoranthene) that are produced by diesel engines (Alves et al., 2017). This result is not surprising, given the proximity of the sampling site to important main traffic routes. Factor 2 described 10.8% of the total variance, exhibiting a high loading for perylene. Nowadays, perylenes are used as high-performance dyes and pigments in several chemical industries (Greene, 2009). Factor 3 explained 9.14% of the total variance, with high contributions from chrysene and benzo[a]anthracene, which are dominant PAHs in biomass burning emissions (Gonçalves et al., 2011).

Table 2. Factor loadings of principal component analysis applied to the dataset of $PM_{2.5}$-bound PAHs.

	Component		
	1	2	3
Naphthalene	**0.64**	**0.64**	-0.07
Acenaphthylene	0.32	0.59	0.19

Acenaphthene	0.54	**0.64**	0.53
Fluorene	**0.92**	0.29	0.13
Chrysene	0.09	0.01	**0.97**
Benzo[a]anthracene	**0.64**	0.28	**0.66**
Benzo[b]fluoranthene	**0.80**	0.48	0.16
Benzo[k]fluoranthene	**0.91**	-0.01	0.31
Benzo[e]pyrene	**0.91**	0.19	0.20
Benzo[a]pyrene	**0.85**	0.37	0.21
Perylene	-0.31	**0.71**	0.02
Indeno[1,2,3-cd]pyrene	**0.84**	0.15	0.47
Dibenzo[a,h]anthracene	**0.88**	0.29	0.20
Benzo[g,h,i]perylene	**0.92**	-0.13	-0.01
Variance (%)	66.1	10.8	9.14
Source	Vehicle emissions	Industry	Biomass burning

Principal components with factor loading higher than 0.6 are shown in bold

Extraction method: principal component analysis

Rotation method: varimax with Kaiser normalisation

Oxygenated organic compounds

In addition to PAHs, many other organic constituents were detected, including anhydrosugars, phenolic compounds, aromatic ketones, glycerol derivatives, aliphatic alcohols, sterols, and aromatic, carboxylic and dicarboxylic acids (Table 3). The complete list can be found in the supplementary material (Table S1). Homologous series of *n*-alkanols (C_{10}-C_{30}) and *n*-alkanoic acids (C_8-C_{28}) with a dominance of even carbon numbers were detected in the aerosol samples. Plant waxes are characterised by even-over-odd carbon number preference for high molecular weight *n*-alkanes ($\geqslant$20), whereas low molecular weight homologues are mainly produced by anthropogenic emissions, although microbial contributions can also be considered. The distributions of *n*-alkanoic acids peaked at C_{18}, followed by C_{16}, which displayed and excellent interrelationship ($r = 0.973$, $p < 0.001$), suggesting common origins. Both compounds have similar pollution roses, pointing to sources spread across the various sectors (Fig. 6). Minor amounts of odd chain length homologues were registered. It has been argued that leaf litter with abundant fatty acids can undergo selective degradation by microorganisms on the soil surfaces, such as microbial α-oxidation of even-carbon numbered homologues, leading to the production of odd-chained relatives (Matsumoto et al., 2007). Since the sampling campaign of this study was carried out in the fall, microbial oxidative processes of leaf litter may, in fact, have contributed to the detection of odd-chain fatty acids. *n*-Alkanols presented maxima at C_{18} and C_{26}, which did not correlate with each other.

Table 3. Concentrations (ng/m^3) of some oxygenated organic compounds detected in $PM_{2.5}$.

	Minimum	Maximum	Average
Fatty alcohols and acids			
1-Octadecanol	0.674	26.0	5.62
1-Hexacosanol	bdl	24.6	6.29
Hexadecanoic acid (palmitic)	31.9	406	84.9
Octadecanoic acid (stearic)	48.3	774	158
cis-9-Octadecenoic acid (oleic)	bdl	8.56	1.30
Monoglycerides			
Monopalmitin	3.97	29.7	14.1
Monostearin	1.95	7.81	4.58
Glycol compounds			
Ethylene glycol	8.87	92.5	22.6
Diethylene glycol	0.374	35.6	10.2
Triethylene glycol	1.28	11.3	60.9
Tetraethylene glycol	1.24	5.73	3.35
Anhydrosugars			
Levoglucosan	29.5	1368	302
Mannosan	1.64	197	41.1
Galactosan	0.725	64.5	15.6
Lignin products			
Vanillin	bdl	5.75	1.45
Vanillic acid	bdl	8.25	1.78
Syringic acid	bdl	14.5	3.20
o-Coumaric acid	1.86	11.4	5.08
p-Coumaric acid	bdl	10.7	3.45
Cinnamic acid	bdl	29.9	2.64
Other biomass burning tracers			
β-Sitosterol	bdl	4.66	1.08
Dehydroabietic acid	bdl	69.1	17.4
Plastic precursors or additives			
Terephthalic acid	1.12	181	54.6
Oxidised Irgafos 168	91.6	1710	327
Aromatic ketones			
2,6-Di-tert-butyl-1,4-benzoquinone	10.8	1231	115
7,9-Di-tert-butyl-1-oxaspiro[4.5]deca-6,9-diene-2,8-dione	bdl	231	27.6
SOA products			
2-Methylglyceric acid oligomers	2.09	1697	241
Pinonic acid	bdl	2.37	0.433
Pinic acid	bdl	57.7	6.61
Pinanediol	bdl	7.72	2.25

Glycerol	10.3	157	39.6
Meso-erythritol	0.701	30.3	8.53
Short chain aliphatic, aromatic, hydroxy-, dihydroxy- and diacids			
4-Hydroxybenzoic acid	0.171	15.1	3.06
Benzoic acid	0.0594	3.05	1.00
Levulinic acid (oxopentanoic)	bdl	26.9	9.62
Hydracrylic acid (3-hydroxypropanoic)	0.323	17.2	3.65
Glyceric acid (2,3-dihydroxypropanoic)	0.578	10.4	3.62
Glycolic acid (2-hydroxyethanoic)	bdl	217	46.7
4-Deoxy-erythronic acid (2,3-dihydroxybutanoic)	6.33	74.2	17.6
Succinic acid (butanedioic)	bdl	139	33.8
Oxalic acid (ethanedioic)	9.56	312	83.1
Malic acid (hydroxybutanedioic)	bdl	19.9	3.99
Azelaic acid (nonanedioic)	bdl	37.4	10.8

bdl – below detection limit

Monopalmitin and monostearin, present in all $PM_{2.5}$ samples, have been described as abundant compounds in fumes from food cooking, especially meat (Alves et al., 2021a). These glyceridic compounds showed weak correlations with palmitic and oleic acids, also referred to as cooking markers, indicating different emission processes. These two unsaturated acids can originate from other sources, such as biomass combustion (Alves et al., 2011; Gonçalves et al., 2011) and traffic (Alves et al., 2021b). Monopalmitin and monostearin, on the other hand, can also be found in the composition of particles from brake wear (Alves et al., 2021b). Oleic acid is simultaneously emitted with its saturated homologue, stearic acid. The oleic-to-stearic acid ratio documented for several sources (cooking, road dust, wood combustion) range from 0.11 to 13 (Robinson et al., 2006, and references therein). In the present study, much lower ratios were obtained (0.001-0.088, avg = 0.033), suggesting other sources and/or photochemical depletion of oleic acid. When oleic acid is attacked by ozone, nonanoic acid is one of the products. However, a weak correlation between $C_{18:1}$ and C_9 was observed, pointing to biogenic sources of nonanoic acid. Among alkanoic acids, the dominance of stearic acid may be related to the manufacture of PVC or other plastics in the industrial complex. Currently, the most common metal soaps used as thermal stabilisers for PVC include Zn and Ca stearates, which are produced by heating stearic acid. Oleic acid may also have an industrial origin, as suggested by its pollution rose. It is used as emulsifier in metalworking fluids and surface coatings, as rubber processing agent and as PVC heat costabiliser (Ashford, 1994).

Ethylene glycol (EG) was present in all $PM_{2.5}$ samples, together with its related oligomers (di-, tri- and tetra-EG). Because of their polar and hygroscopic characteristics, these synthetic organic compounds are rapidly absorbed after entering the upper respiratory passages, exerting acute toxicity characterised by central nervous system depression and metabolic acidosis in humans (Fowles et al.,

2017). EGs are commonly added as plasticiser ingredients in the manufacture of PVC and other thermoplastic polymers. Thus, their detection in fine inhalable particles is, at least in part, linked to these industrial processes. However, this compound can also be emitted by traffic. Although most vehicular organic compounds are from evaporation and incomplete combustion of fuels and lubricating oils, engine coolants represent another possible vehicular emission source. EG is the most common engine coolant. EG emissions from on-road vehicles have been previously measured in the Caldecott Tunnel near San Francisco (Wood et al., 2015). According to the pollution rose, in Estarreja, the EG compounds seem to originate in all quadrants from which the winds blow, indicating contributions not only from the industrial complex, but also from the road network.

Another organic compound detected at relatively high concentrations with a probable origin in the industrial pole is terephthalic acid. It is a commodity chemical, mainly used as a precursor to polyethylene terephthalate (PET), one of the products synthesised in the complex. Oxidised Irgafos 168 (tris(2,4-ditert-butylphenyl) phosphate), also detected at relatively high concentrations, is one of the common antioxidants widely used in the industry to protect polymers from aging and oxidation. Besides originating in the industrial complex, this organophosphorus compound may be associated with non-exhaust emissions, as it was recently detected as a component of brake wear particles (Alves et al., 2021b). In addition to the industrial source, this origin in traffic is proven by the high concentrations spread across the various sectors of the pollution rose, according to the extensive road network that covers Estarreja.

Some aromatic ketones were present in the $PM_{2.5}$ samples. Due to its abundance, 2,6-di-tert-butyl-1,4-benzoquinone stands out. It has been reported that PAH quinone derivatives are more toxic than their parent PAHs, as they do not require enzymatic activation, thus acting as direct mutagens and/or carcinogens. Like their parent PAHs, quinones may be released into the atmosphere through incomplete combustion processes. Gaseous and heterogeneous atmospheric processing of PAHs can yield further quinone products through photochemical reactions involving atmospheric oxidants (OH, NO_3 and O_3) or through biological transformations (Delgado-Saborit et al., 2013, and references therein). This quinone was previously observed in particulate matter samples collected at a trafficked roadside in Birmingham (Delgado-Saborit et al., 2013). Given that the average concentration (1900 pg/m^3) at the British site was significantly lower than those of the present study, it is assumed that other emission sources and more active photochemical processes have taken place in Estarreja. An origin in the industrial complex should not be overlooked, since this quinone was recently described as a synthetic phenolic antioxidant widely used in various industrial and commercial products to retard oxidative reactions and lengthen product shelf life (Liu and Mabury, 2020). In fact, the highest concentrations were registered for winds emanating from the NW sector, in which the industrial complex is located. 7,9-Di-tert-butyl-1-oxaspiro[4.5]deca-6,9-diene-2,8-dione was another aromatic ketone present in almost all samples. Although it can be extracted from marine algae and some plant species, the presence in the atmosphere is mainly due to its use in the manufacture of plastic materials. It was previously

observed in aerosol particles from Raipur by Giri et al. (2013), who pointed out an origin in plastic burning and fugitive emissions. The mean value of the present study (18.5 ng/m^3) is higher than that obtained in that industrial city of India (5.2 ng/m^3).

Levoglucosan (L), accompanied by its stereoisomers, mannosan (M) and galactosan (G), were detected in all samples. These anhydrosugars originate from thermal depolymerisation of cellulose and hemicelluloses to monosaccharides, followed by a dehydrolysis reaction. Levoglucosan has been widely used as a marker for biomass burning processes (Vicente and Alves, 2018). The pollution rose showed higher levoglucosan concentrations for lower wind speeds across all sectors, indicating that biomass burning is a widespread phenomenon at the local level. An average value of 18 was obtained for the L/M ratio, suggesting combustion processes involving predominantly angiosperms, a group often referred to as hardwoods (e.g., eucalypt). Gonçalves et al. (2010) reported ratios in the range from 10 to 35 for hardwoods and a value of 3 for softwood in PM_{10} emissions from woodstove combustion of logs from trees representative of the Portuguese forest. Considering that the nearby forest is mainly composed of eucalypt, the levoglucosan fraction in $PM_{2.5}$ of 0.173 reported by Gonçalves et al. (2011) for the residential combustion of this wood species was taken to roughly estimate the contribution of biomass burning. Thus, the following relationship was used:

$$PM_{2.5} \text{ from biomass burning} = \text{levoglucosan} \times 5.8 \quad (5)$$

It was estimated that, on average, biomass burning accounted for 13.8% of the $PM_{2.5}$ concentrations. Due to the extensive use of residential wood combustion appliances for heating, much higher contributions have been reported for other regions in Portugal for the winter period (Amato et al., 2016; Gonçalves et al., 2021). Levoglucosan was negatively correlated with temperature ($r = -0.740$, $p < 0.001$), indicating that there is more need to burn biofuels for home heating with colder weather. It is necessary to take into account that the small town is surrounded by agricultural areas, so field burning of crop and pruning residues may have also contributed to the $PM_{2.5}$ levels.

Lignin is a biopolymer derived from three main aromatic alcohols: p-coumaryl, coniferyl and sinapyl. The pyrolysis products of these aromatic alcohols are denominated as coumaryl, vanillyl, and syringyl moieties. Hardwood (angiosperms) burning mainly generates syringyl and vanillyl moieties because their lignin is enriched in sinapyl alcohol precursors. Combustion of softwoods (gymnosperms) instead produces primarily vanillyl moieties since these species have high proportions of coniferyl alcohol products and minor amounts of sinapyl alcohol. In grasses (Gramineae), p-coumaryl alcohol is the dominant lignin unit. Several phenolic compounds from lignin combustion were detected, including vanillin, vanillic acid, syringic acid, coumaric acid and cinnamic acid. These compounds correlated well with levoglucosan ($r = 0.849$-0.875, $p < 0.001$). β-Sitosterol, a general biomass burning tracer present in smoke from a variety of vegetation types (Vicente and Alves, 2018), was also found in most

of the aerosol samples. Other biomass burning products with good correlation with levoglucosan were 4-hydroxybenzoic acid ($r = 0.866$, $p < 0.001$) and dehydroabietic acid ($r = 0.915$, $p < 0.001$).

The two most abundant biogenic volatile organic compounds (VOC) emitted into the atmosphere are isoprene and methane. Isoprene reacts with OH, NO_3 and O_3 leading to the formation of less volatile secondary organic aerosol (SOA) via condensation or uptake onto particulates through cascading oxidative pathways (Carlton et al., 2009). Isoprene-derived SOA are broadly produced in highly forested regions. *Eucalyptus* spp., one of the dominant trees in the Estarreja region, are among the highest isoprene emitting plants (Loreto and Delfine, 2000). In this study, several 2-methylglyceric acid oligomers formed from the photooxidation of isoprene were detected (Szmigielski et al., 2007). The mass spectra of TMS ethyl ester derivatives of 2-methylglyceric acid are characterised by a dominant ion at *m/z* 219. Other SOA constituents present in $PM_{2.5}$ included α/β-pinene photooxidation products, such as pinonic and pinic acids and pinanediol (Bilde and Pandis, 2001). Glycerol and meso-erythritol, which have been described as photodecomposition products of 1,3-butadiene in air containing nitric oxide (Angove et al., 2006), were also observed in the aerosol samples. This VOC precursor is emitted by traffic and industrial processes.

Short chain aliphatic, aromatic, hydroxy-, dihydroxy- and diacids are emitted in small amounts as primary constituents by many sources, but a large part of the concentrations in particulate matter is due to secondary formation. Some of these acids (e.g., suberic) presented higher concentrations when the $PM_{2.5}$ samples were impacted by winds from the 4th quadrant, suggesting the contribution from industrial processes. Benzoic acid was one of the aromatic acids encountered in all samples. Although it can be emitted in the combustion of biomass, the fact that it did not correlate with levoglucosan is indicative of other formation processes. It has been reported as a secondary product of photochemical degradation of toluene emitted from anthropogenic sources. Besides road traffic, in Estarreja, the chemical industrial complex is a known source of toluene and other aromatic VOCs. Other aerosol compounds that have been described from the photooxidation of toluene and NO_x in smog chamber experiments (White et al., 2014), also observed in the present study, included levulinic, glyceric, succinic, oxalic and malic acids. Glycolic acid was one of the most abundant hydroxyacids. It has been documented as either anthropogenic or biogenic SOA product from ethylene oxidation (Huang et al., 2011) or isoprene through in-cloud processing (Lim et al., 2005), respectively. Hydracrylic acid (3-hydroxypropanoic acid) was also found in all samples. Possible precursors of this acid include (Z)-3-hexen-1-ol (also known as leaf alcohol), which is emitted by vegetation, simpler unsaturated alcohols (e.g., 3-buten-1-ol), as well as 1,3-propanediol (Pun et al., 2000). Another ever-present constituent was 2,3-dihydroxybutanoic acid. It can be formed by oxidation of the double bond of crotonaldehyde, a VOC with many biogenic and anthropogenic sources, to a dihydroxy derivative (Shalamzari et al., 2013).

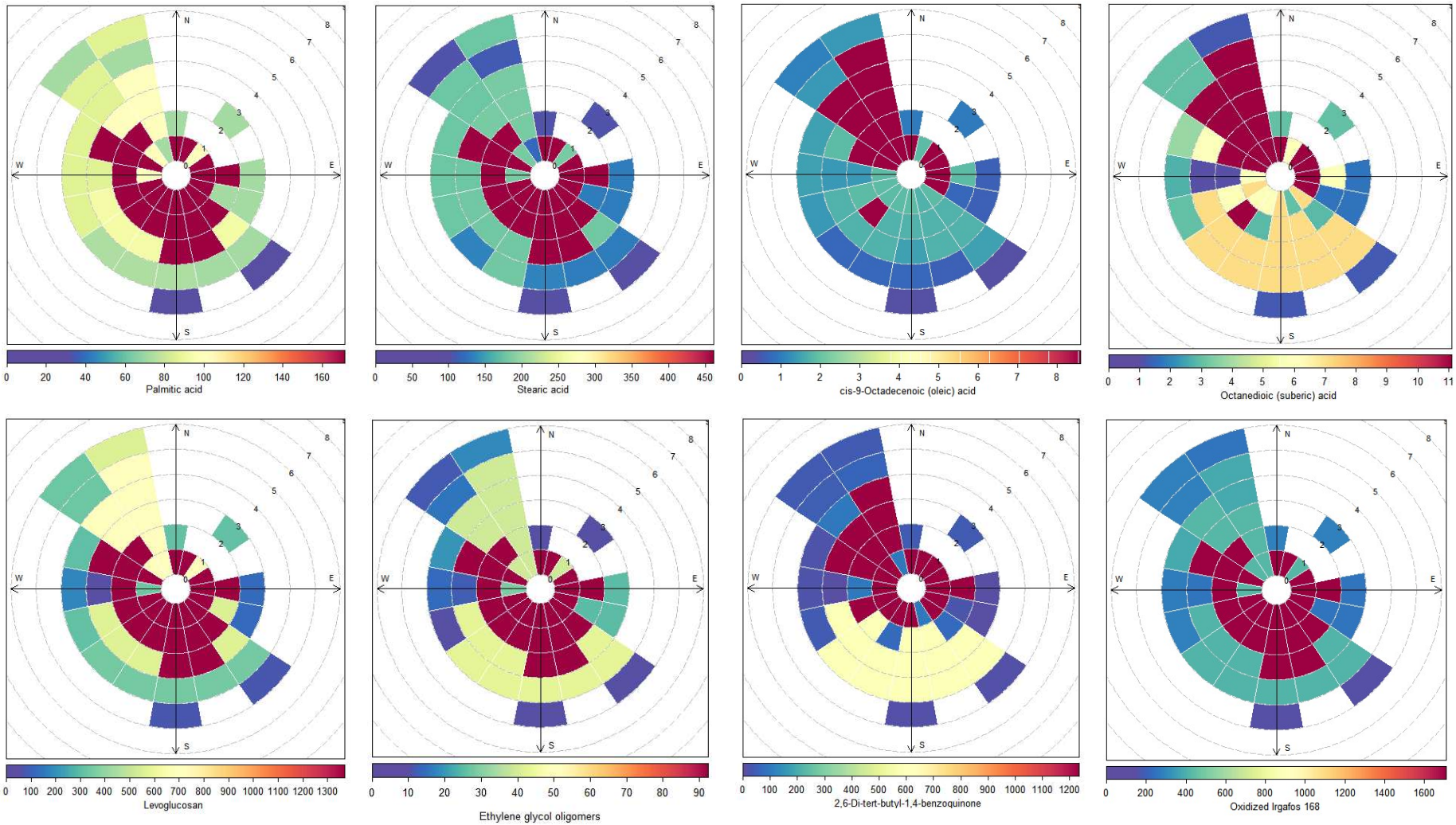

Fig. 6. Pollution roses for some oxygenated organic compounds detected in $PM_{2.5}$. Wind speeds and concentrations are given in m/s and ng/m^3, respectively.

Noncarcinogenic and carcinogenic risks by inhalation

Carcinogenic risks (average and ranges) associated with exposure to $PM_{2.5}$-bound elements are presented in Table 4. Negligible risks ($<1\times10^{-6}$) were found for all the individual elements studied, apart from hexavalent chromium, whose risks ranged from 0.00 to 6.89×10^{-5}. The average cumulative carcinogenic risks of $PM_{2.5}$-bound metals exceeded the USEPA threshold of 1×10^{-6}. The major contributors to carcinogenic risks of the population exposed in the city of Estarreja were Cr(VI) (average contribution of 56%) and As (average contribution of 16%). However, it is necessary to keep in mind that the risks are expected to be higher if other exposure pathways (dermal absorption and ingestion) are taken into account.

Table 4. Incremental lifetime cancer risk of inhalation exposure to carcinogenic $PM_{2.5}$-bound metals.

Element	Average	Range (min - max)
Cr(VI)	9.60×10^{-6}	0.00 - 6.89×10^{-5}
As	4.53×10^{-7}	0.00 - 2.62×10^{-6}
Pb	4.54×10^{-8}	3.84×10^{-9} - 1.09×10^{-7}
Co	1.73×10^{-7}	0.00 - 7.47×10^{-7}
Cd	1.09×10^{-7}	0.00 - 5.77×10^{-7}
Ni	1.77×10^{-7}	0.00 - 6.97×10^{-7}
ΣTP	1.06×10^{-5}	1.65×10^{-8} - 6.95×10^{-5}

IUR: arsenic (4.3×10^{-3} (μg m^{-3})$^{-1}$), lead (1.2×10^{-5} (μg m^{-3})$^{-1}$), chromium (VI) (8.4×10^{-2} (μg m^{-3})$^{-1}$), cobalt (9×10^{-3} (μg m^{-3})$^{-1}$), cadmium (1.8×10^{-3} (μg m^{-3})$^{-1}$) and nickel (2.6×10^{-4} (μg m^{-3})$^{-1}$).

In the present study, the noncarcinogenic risks were estimated based on the concentrations of thirteen elements. The additive noncarcinogenic risk was below the USEPA threshold of 1 (Table 5), indicating that adverse effects are not likely to occur. Nevertheless, it should not be forgotten that some major elements, possibly present in the particles, have not been analysed, so the risk may be higher.

Table 5. Non-carcinogenic risks via inhalation exposure to $PM_{2.5}$-bound elements.

Element	Average	Range (min - max)
Ni	1.07×10^{-11}	0.00 – 4.21×10^{-11}
Cd	1.21×10^{-12}	0.00 – 6.41×10^{-12}
Co	1.16×10^{-13}	0.00 – 4.98×10^{-13}
Cr	8.00×10^{-11}	0.00 – 5.74×10^{-10}

As	1.58×10^{-12}	$0.00 – 9.14\times10^{-12}$
Pb	7.56×10^{-10}	$6.40\times10^{-11} – 1.81\times10^{-9}$
V	2.13×10^{-10}	$0.00 – 8.89\times10^{-10}$
Cu	6.53×10^{-7}	$1.48\times10^{-7} – 2.14\times10^{-6}$
Zn	2.22×10^{-5}	$4.32\times10^{-6} – 4.67\times10^{-5}$
Se	1.17×10^{-9}	$0.00 – 2.96\times10^{-9}$
Sr	1.13×10^{-6}	$2.42\times10^{-7} – 2.96\times10^{-6}$
Zr	1.25×10^{-10}	$0.00 – 6.89\times10^{-10}$
Ba	1.20×10^{-9}	$1.44\times10^{-10} – 2.55\times10^{-9}$
ΣTHQ	2.40×10^{-5}	$6.56\times10^{-6} – 4.91\times10^{-5}$

R_fC: Nickel oxide (2.00×10^{-5} mg m^{-3}), cadmium (2.00×10^{-5} mg m^{-3}), cobalt (6.00×10^{-6} mg m^{-3}), chromium (1.00×10^{-4} mg m^{-3}), arsenic (1.50×10^{-5} mg m^{-3}), lead (2.00×10^{-4} mg m^{-3}), vanadium (1.00×10^{-4} mg m^{-3}), copper (1.40×10^{-1} mg m^{-3}), zinc (1.05×10^{0} mg m^{-3}), selenium (2.00×10^{-2} mg m^{-3}), strontium (2.00×10^{0} mg m^{-3}), zirconium (2.80×10^{-4} mg m^{-3}) and barium (5.00×10^{-4} mg m^{-3}).

The lifetime cancer risk associated with exposure to $PM_{2.5}$-bound PAHs through the inhalation pathway was estimated to range from 5.6×10^{-11} to 3.4×10^{-6}, averaging 6.7×10^{-7}, which represents a negligible CR. Higher cancer risks have been reported for other industrialised areas around the world. A cancer risk of 2.8×10^{-5} was obtained for $PM_{2.5}$-bound PAHs in an urban-industrial area in Pretoria, South Africa, composed of several facilities, including small boilers, two power plants and metallurgies (Morakinyo et al., 2020). A cancer risk of 2.8×10^{-5} was reported for PM_{10}-bound PAHs collected in the vicinity of a heavily industrialised site in Greece, where large crude oil refineries and over 300 industrial plants are located, comprising metallurgical processes, cement, chemical and food production, shipyards, etc. (Koukoulakis et al., 2020). Using the global high-resolution PKU-FUEL-2007 inventory and the Community Multiscale Air Quality (CMAQ) model, Han et al. (2020) simulated the concentrations of PAHs in China and estimated the associated health risks. The incremental lifetime cancer risk was found to be > 5×10^{-4} in many urban and industrial areas, especially those where coal combustion, oil and gas related activities are concentrated.

Conclusions

The composition of $PM_{2.5}$ sampled in a small town in the vicinity of a large industrial complex was investigated. Most of the mass was composed of carbonaceous material (25.2% OC and 11.4% EC), which included a wide range of organic compounds of different polarities. Multiple compounds known for their toxicity (e.g., PAHs, alkyl-PAHs, aromatic ketones, ethylene glycol, etc.) were detected. It was

estimated that 2-3 ring PAHs were almost entirely in the gas phase, while 4 ring congeners were partitioned between the gas (54%) and the particulate phase (46%), and 5-6-membered rings were mainly in the particulate form. $PM_{2.5}$-bound PAHs originated in traffic (66%), industrial (11%) and biomass burning (9%) emissions. The latter source was estimated to contribute to 14% of $PM_{2.5}$ concentrations, while 20% of the aerosol mass was secondarily formed from both biogenic and anthropogenic precursors. Very or extremely high enrichment factors suggested anthropogenic origins for Pb, Cd, Zn, Cu, Sn, B, Se, Bi, Sb and Mo. The pollution roses indicated that some constituents, especially those related to metallurgical processes and the production of plastics and glass-ceramics, peaked their concentrations when the winds blew from the 4th quadrant, in which the industrial complex is located. However, many $PM_{2.5}$-bound components revealed sources spread across the various sectors, pointing to traffic emissions due to the high density of motorways and main roads passing through the municipality.

The cancer and noncancer risks from inhalation of $PM_{2.5}$-bound PAHs and elements, respectively, were found to be negligible, but the cumulative cancer risk for metals, especially due to chromium and arsenic, was beyond the acceptable guideline. This risk, together with the detection of various organic substances with recognised toxicity, lead to recommend the adoption of mitigation measures focused on the main emission sources. The industry is a very heterogeneous sector comprising many sub-sectors, which should require specific carbon footprint assessments and the adoption of the best available technologies to reduce upstream, downstream and in-process emissions. The European Pollutant Release and Transfer Register (E-PRTR) emission data, as well as the permit conditions and environmental inspections set by the Industrial Emissions Directive should be revised with the inclusion of new pollutants. It is also necessary to implement regulatory and voluntary programmes to reduce emissions from burning biomass, including incentives for replacing old and inefficient combustion equipment, education and outreach tools, air quality forecasting and public notification systems, among others. Agricultural burning must be replaced by other waste management practices, namely composting or crushing and incorporation of leftovers into the soil. Although the problem of road traffic is difficult to solve in the short term, in the future, in this and other regions, territorial planning policies with a better spatial distribution of industrial conurbations and road networks are needed.

Although $PM_{2.5}$ levels in the vicinity of the industrial complex reasonably comply with legislation, as the toxicity may depend more on the composition, to complement this chemical characterisation, the phenotypic and metabolic effects of the constituents extracted from $PM_{2.5}$ will be assessed through *in vitro* cellular assays, including the investigation of cellular metabolic activity, secretion of proinflammatory mediators, and expression/secretion of proinflammatory cytokines/chemokines and matrix metalloproteinases.

CRediT authorship contribution statement

Célia Alves: Project administration, Funding acquisition, Conceptualisation, Methodology, Formal analysis, Supervision, Writing – original draft. Margarita Evtyugina: Investigation, Writing – review and editing. Estela Vicente: Investigation, Formal analysis, Writing – review and editing. Ana Vicente: Investigation, Writing – review and editing. Ismael Casotti Rienda: Investigation, Writing – review and editing. Ana Sánchez de la Campa: Investigation, Writing – review and editing. Mário Tomé: Formal analysis, Writing – review and editing. Iola F. Duarte: Project administration, Funding acquisition, Writing – review and editing.

Declaration of competing interest

The authors declare that they have no known competing financial interests or personal relationships that could have appeared to influence the work reported in this paper.

Acknowledgments

The sampling campaign and analytical work were supported by the projects "ATHEROFIT: Phytochemical-based metabolic immunomodulation to prevent/attenuate particulate matter-mediated atherosclerosis" (OHM-Estarreja/2019-2128), funded by LabEx DRIIHM, and "SOPRO: Chemical and toxicological SOurce PROfiling of particulate matter in urban air", POCI-01-0145-FEDER-029574, funded by FEDER, through COMPETE2020 - Programa Operacional Competitividade e Internacionalização (POCI), and by national funds (OE), through FCT/MCTES. Margarita Evtyugina, Estela Vicente and Ismael Casotti Rienda acknowledge, respectively, the grants SFRH/BPD/123176/2016, SFRH/BD/117993/2016 and SFRH/BD/144550/2019 from the Portuguese Foundation for Science and Technology (FCT). Ana Vicente was subsidised by national funds (OE), through FCT, I.P., in the framework contract foreseen in the numbers 4, 5 and 6 of article 23, of the Decree-Law 57/2016, of August 29, changed by Law 57/2017, of July 19. We are also grateful for the support to CESAM (UIDB/50017/2020 & UIDP/50017/2020) and CICECO (UIDB/50011/2020 & UIDP/50011/2020), to FCT/MCTES through national funds, and co-funding by FEDER, within the PT2020 Partnership Agreement and Compete 2020.

References

Acciai, C., Zhang, Z., Wang, F., Zhong, Z., Lonati, G., 2017. Characteristics and source analysis of trace elements in $PM_{2.5}$ in the urban atmosphere of Wuhan in spring. Aerosol Air Qual. Res. 17, 2224–2234. https://doi.org/10.4209/aaqr.2017.06.0207

Adamiec, E., 2017. Chemical fractionation and mobility of traffic-related elements in road environments. Environ. Geochem. Health 39, 1457-1468. https://doi.org/10.1007/s10653-017-9983-9

Agarwal, A.K., Singh, A.P., Gupta, T., Agarwal, R.A., Sharma, N., Rajput, P., Pandey, S.K., Ateeq, B., 2018. Mutagenicity and cytotoxicity of particulate matter emitted from biodiesel-fueled engines. Environ. Sci. Technol. 52, 14496-14507. https://doi.org/10.1021/acs.est.8b03345

Alves C.A., Vicente A.M., Custodio D., Cerqueira M., Nunes T., Pio C., Lucarelli F., Calzolai G., Nava S., Diapouli E., Eleftheriadis K., Querol X., Bandowe B.A.M., 2017. Polycyclic aromatic hydrocarbons and their derivatives (nitro-PAHs, oxygenated PAHs, and azaarenes) in $PM_{2.5}$ from Southern European cities. Sci. Total Environ. 595, 494-504. https://doi.org/10.1016/j.scitotenv.2017.03.256

Alves, C., Evtyugina, M., Vicente, A., Conca, E., Amato, F., 2021b. Organic profiles of brake wear particles. Atmos. Res. 255, 105557. https://doi.org/10.1016/j.atmosres.2021.105557

Alves, C.A., Vicente, A., Monteiro, C., Gonçalves, C., Evtyugina, M., Pio, C., 2011. Emission of trace gases and organic components in smoke particles from a wildfire in a mixed-evergreen forest in Portugal. Sci. Total Environ. 409, 1466-1475. https://doi.org/10.1016/j.scitotenv.2010.12.025

Alves, C.A., Vicente, E.D., Evtyugina, M., Vicente, A.M., Nunes, T., Lucarelli, F., Calzolai G., Nava, S., Calvo, A.I., Alegre, C.D., Oduber, F., Castro, A., Fraile, R., 2020. Indoor and outdoor air quality: A university cafeteria as a case study. Atmos. Pollut. Res. 11, 531-544. https://doi.org/10.1016/j.apr.2019.12.002

Alves, C.A., Vicente, E.D., Evtyugina, M., Vicente, A.M.P., Sainnokhoi, T.A., Kováts, N., 2021a. Cooking activities in a domestic kitchen: Chemical and toxicological profiling of emissions. Sci. Total Environ. 772, 145412. https://doi.org/10.1016/j.scitotenv.2021.145412

Amato, F., Alastuey, A., Karanasiou, A., Lucarelli, F., Nava, S., Calzolai, G., Severi, M., Becagli, S., Gianelle, V.L., Colombi, C., Alves, C., Custódio, D., Nunes, T., Cerqueira, M., Pio, C., Eleftheriadis, K., Diapouli, E., Reche, C., Minguillon, M.C., Manousakas, M.I., Maggos, T., Vratolis, S., Harrison, R.M., Querol, X., 2016. AIRUSE-LIFE plus: a harmonized PM speciation and source apportionment in five southern European cities. Atmos. Chem. Phys. 16, 3289-3309. https://doi.org/10.5194/acp-16-3289-2016

Angove, D.E., Fookes, C.J.R., Hynes, R.G., Walters, C.K., Azzi, M., 2006. The characterisation of secondary organic aerosol formed during the photodecomposition of 1,3-butadiene in air containing nitric oxide. Atmos. Environ. 40, 4597-4607. https://doi.org/10.1016/j.atmosenv.2006.03.046

Ashford, R.D., 1994. Ashford's Dictionary of Industrial Chemicals. Wavelength Publications Ltd., London, England, p. 650.

Benetello, B., Squizzato, S., Hofer, A., Masiol, M., Khan, M.B., Piazzalunga, A., Fermo, P., Formenton, G.M., Rampazzo, G., Pavoni, B., 2017. Estimation of local and external contributions of biomass

burning to $PM_{2.5}$ in an industrial zone included in a large urban settlement. Environ. Sci. Pollut. Res. 24, 2100-2115. https://doi.org/10.1007/s11356-016-7987-0

Besis, A., Tsolakidou, A., Balla, D., Samara, C., Voutsa, D., Pantazaki, A., Choli-Papadopoulou, T., Lialiaris, T.S., 2017. Toxic organic substances and marker compounds in size-segregated urban particulate matter - Implications for involvement in the *in vitro* bioactivity of the extractable organic matter. Environ. Pollut. 230, 758-774. https://doi.org/10.1016/j.envpol.2017.06.096

Bilde, M., Pandis, S.N., 2001. Evaporation rates and vapor pressures of individual aerosol species formed in the atmospheric oxidation of α- and β-pinene. Environ. Sci. Technol. 35, 3344-3349. https://doi.org/10.1021/es001946b

Bowe, B., Xie, Y., Yan, Y., Al-Aly, Z., 2019. Burden of cause-specific mortality associated with $PM_{2.5}$ air pollution in the United States. JAMA Network Open 2, e1915834. https://doi.org/10.1001/jamanetworkopen.2019.15834

Brazdil, J.F., 2017. A critical perspective on the design and development of metal oxide catalysts for selective propylene ammoxidation and oxidation. Appl. Catal. A Gen. 543, 225–233. https://doi.org/10.1016/j.apcata.2017.06.022

Carlton, A.G., Wiedinmyer, C., Kroll, J.H., 2009. A review of secondary organic aerosol (SOA) formation from isoprene. Atmos. Chem. Phys. 9, 4987-5005. https://doi.org/10.5194/acp-9-4987-2009

Casal, C.S., Arbilla, G., Corrêa, S.M., 2014. Alkyl polycyclic aromatic hydrocarbons emissions in diesel/biodiesel exhaust. Atmos. Environ. 96, 107-116. https://doi.org/10.1016/j.atmosenv.2014.07.028

Chao, S., Liu, J., Chen, Y., Cao, H., Zhang, A., 2019. Implications of seasonal control of $PM_{2.5}$-bound PAHs: An integrated approach for source apportionment, source region identification and health risk assessment. Environ. Pollut. 247, 685-695. https://doi.org/10.1016/j.envpol.2018.12.074

Delgado-Saborit, J.M., Alam, M.S., Pollitta, K.J.G., Stark, C., Harrison, R.M., 2013. Analysis of atmospheric concentrations of quinones and polycyclic aromatic hydrocarbons in vapour and particulate phases. Atmos. Environ. 77, 974-982. https://doi.org/10.1016/j.atmosenv.2013.05.080

Draxler, R.R., Rolph, G.D., 2015. HYSPLIT (HYbrid Single-Particle Lagrangian Integrated Trajectory) Model Access via NOAA ARL READY Website (http://www.arl.noaa.gov/HYSPLIT.php) on February 24th, 2015. NOAA Air Resources Laboratory, College Park.

EEA, 2020. Air quality in Europe - 2020 report. EEA Report No 9/2020. European Environment Agency. Publications Office of the European Union, Luxembourg.

Elzein, A., Stewart, G.J., Swift, S.J., Nelson, B.S., Crilley, L.R., Alam, M.S., Reyes-Villegas, E., Gadi, R., Harrison, R.M., Hamilton, J.F., Lewis, A.C., 2020. A comparison of $PM_{2.5}$-bound polycyclic aromatic hydrocarbons in summer Beijing (China) and Delhi (India). Atmos. Chem. Phys. 20, 14303-14319. https://doi.org/10.5194/acp-20-14303-2020

Fang, B., Zhang, L., Zeng, H., Liu, J., Yang, Z., Wang, H., Wang, Q., Wang, M., 2020. $PM_{2.5}$-bound polycyclic aromatic hydrocarbons: Sources and health risk during non-heating and heating periods (Tangshan, China). Int. J. Environ. Res. Public Health 17, 483. https://doi.org/10.3390/ijerph17020483

Ferrari, C.P., Hong, S., Van De Velde, K., Boutron, C.F., Rudniev, S.N., Bolshov, M., Chisholm, W., Rosman, K.J.R., 2000. Natural and anthropogenic bismuth in Central Greenland. Atmos. Environ. 34, 941–948. https://doi.org/10.1016/S1352-2310(99)00257-5

Figueiredo, M.L., Monteiro, A., Lopes, M., Ferreira, J., Borrego, C., 2013. Air quality assessment of Estarreja, an urban industrialized area, in a coastal region of Portugal. Environ. Monit. Assess. 185, 5847-5860. https://doi.org/10.1007/s10661-012-2989-y

Fowles, J., Banton, M., Klapacz, J., Shen, H., 2017. A toxicological review of the ethylene glycol series: Commonalities and differences in toxicity and modes of action. Toxicol. Lett. 278, 66-83. https://doi.org/10.1016/j.toxlet.2017.06.009

Gao, B., Wang, X.M., Zhao, X.Y., Ding, X., Fu, X.X., Zhang, Y.L., He, Q.F., Zhang, Z., Liu, T.Y., Huang, Z.Z., Chen, L.G., Peng, Y., Guo H., 2015. Source apportionment of atmospheric PAHs and their toxicity using PMF: Impact of gas/particle partitioning. Atmos. Environ. 103, 114-120. https://doi.org/10.1016/j.atmosenv.2014.12.006

GBD 2019 Risk Factors Collaborators, 2020. Global burden of 87 risk factors in 204 countries and territories, 1990–2019: a systematic analysis for the Global Burden of Disease Study 2019. Lancet 396, 1223-1249. https://doi.org/10.1016/S0140-6736(20)30752-2

Giria, B., Patel, K.S., Jaiswal, N.K., Sharma, S., Ambade, B., Wang, W., Simonich, S.L.M., Simoneit B.R.T., 2013. Composition and sources of organic tracers in aerosol particles of industrial central India. Atmos. Res. 120-121, 312-324. https://doi.org/10.1016/j.atmosres.2012.09.016

Gonçalves, C., Alves, C., Evtyugina, M., Mirante, F., Pio, C., Caseiro, A., Schmidl, C., Bauer, H., Carvalho, F.P., 2010. Characterisation of PM_{10} emissions from woodstove combustion of common woods grown in Portugal. Atmos. Environ. 44, 4474–4480. https://doi.org/10.1016/j.atmosenv.2010.07.026

Gonçalves, C., Alves, C., Fernandes, A.P., Monteiro, C., Tarelho, L., Evtyugina, M., Pio, C., 2011. Organic compounds in $PM_{2.5}$ emitted from fireplace and woodstove combustion of typical Portuguese wood species. Atmos. Environ. 45, 4533-4545. https://doi.org/10.1016/j.atmosenv.2011.05.071

Gonçalves, C., Casotti Rienda, I., Pina, N., Gama, G., Nunes, T., Tchepel, O., Alves, C., 2021. PM_{10}-bound sugars: chemical composition, sources and seasonal variations. Atmosphere 12, 194. https://doi.org/10.3390/atmos12020194

González, N., Esplugas, R., Marquès, M., Domingo, J.L., 2021. Concentrations of arsenic and vanadium in environmental and biological samples collected in the neighborhood of petrochemical industries:

A review of the scientific literature. Sci. Total Environ. 771. https://doi.org/10.1016/j.scitotenv.2021.145149

Greene, M., 2009. Perylene Pigments Chapter 9, in: Faulkner, E.B., Schwartz, R.J. (Eds.), High Performance Pigments, Second Edition, Wiley-VCH Verlag GmbH & Co. KGaA, Weinheim, pp. 261-274.

Grigoratos, T., Martini, G., 2015. Brake wear particle emissions: a review. Environ. Sci. Pollut. Res. 22, 2491-2504. https://doi.org/10.1007/s11356-014-3696-8

Han, F., Guo, H., Hu, J., Zhang, J., Ying, Q., Zhang, H., 2020. Sources and health risks of ambient polycyclic aromatic hydrocarbons in China. Sci. Total Environ. 698, 134229. https://doi.org/10.1016/j.scitotenv.2019.134229

Han, W., Zhang, M., Li, D., Dong, T., Ai, B., Dou, J., Sun, H., 2019. Design and synthesis of a new mannitol stearate ester-based aluminum alkoxide as a novel tri-functional additive for poly(vinyl chloride) and its synergistic effect with zinc stearate. Polymers (Basel). 11. https://doi.org/10.3390/polym11061031

HEI, 2020. State of Global Air 2020. Special Report. Health Effects Institute. Boston, MA. URL: https://www.stateofglobalair.org/ (accessed 18/03/2021).

Hu, R., Liu, G., Zhang, H., Xue, H., Wang, X., 2017. Levels and sources of PAHs in airborne $PM_{2.5}$ of Hefei City, China. Bull. Environ. Contam. Toxicol. 98, 270-276. https://doi.org/10.1007/s00128-016-2019-9

Huang, X.H.H., Ip, H.S.S., Yu, J.Z., 2011. Secondary organic aerosol formation from ethylene in the urban atmosphere of Hong Kong: A multiphase chemical modeling study. J. Geophys. Res. 116, D03206. https://doi.org/10.1029/2010JD014121

IARC, 2013. Air Pollution and Cancer. IARC Scientific Publication Nº 161. Straif, K., Cohen, A., Samet, J. (Eds.). International Agency for Research on Cancer, WHO Press, World Health Organization. Geneva, Switzerland. URL: https://www.iarc.who.int/wp-content/uploads/2018/07/AirPollutionandCancer161.pdf (accessed 18/03/2021).

Jia, Y.Y., Wang, Q., Liu, T., 2017. Toxicity research of $PM_{2.5}$ compositions *in vitro*. Int. J. Environ. Res. Public Health 14, 232. https://doi.org/10.3390/ijerph14030232

Kazakos, V., Luo, Z., Ewart, I., 2020. Quantifying the health burden misclassification from the use of different $PM_{2.5}$ exposure Tier models: A case study of London. Int. J. Environ. Res. Public Health 17, 1099. https://doi.org/10.3390/ijerph17031099

Kot, F.S., 2009. Boron sources, speciation and its potential impact on health. Rev. Environ. Sci. Biotechnol. 8, 3-28. https://doi.org/10.1007/s11157-008-9140-0

Koukoulakis, K.G., Kanellopoulos, P.G., Chrysochou, E., Costopoulou, D., Vassiliadou, I., Leondiadis, L., Bakeas, E., 2020. Atmospheric concentrations and health implications of PAHs, PCBs and PCDD/Fs in the vicinity of a heavily industrialized site in Greece. Appl. Sci. 10, 9023. https://doi.org/10.3390/app10249023

Lim, H.J., Carlton, A.G., Turpin, B.J., 2005. Isoprene forms secondary organic aerosol through cloud processing: Model simulations. Environ. Sci. Technol. 39, 4441-4446. https://doi.org/10.1021/es048039h

Liu, R., Mabury, S.A., 2020. Synthetic phenolic antioxidants: A review of environmental occurrence, fate, human exposure, and toxicity. Environ. Sci. Technol. 54, 11706-11719. https://doi.org/10.1021/acs.est.0c05077

Liu, X., Schnelle-Kreis, J., Schloter-Hai, B., Ma., L., Tai, P., Cao, X., Yu, C., Adam, T., Zimmermann, R., 2019. Analysis of PAHs associated with PM_{10} and $PM_{2.5}$ from different districts in Nanjing. Aerosol Air Qual. Res. 19, 2294-2307. https://doi.org/10.4209/aaqr.2019.06.0301

Loreto, F., Delfine, S., 2000. Emission of isoprene from salt-stressed *Eucalyptus globulus* leaves. Plant Physiol. 123, 1605-1610. https://doi.org/10.1104/pp.123.4.1605

Matsumoto, K., Kawamura, K., Uchida, M., Shibata, Y., 2007. Radiocarbon content and stable carbon isotopic ratios of individual fatty acids in subsurface soil: implication for selective microbial degradation and modification of soil organic matter. Geochem. J. 41, 483-492. https://doi.org/10.2343/geochemj.41.483

Morakinyo, O.M., Mukhola, M.S., Mokgobu, M.I., 2020. Concentration levels and carcinogenic and mutagenic risks of $PM_{2.5}$-bound polycyclic aromatic hydrocarbons in an urban-industrial area in South Africa. Environ. Geochem. Health 42, 2163-2178. https://doi.org/10.1007/s10653-019-00493-2

Moreno, T., Querol, X., Alastuey, A., Viana, M., Salvador, P., Sánchez de la Campa, A., Artiñano, B., de la Rosa, J., Gibbons, W., 2006. Variations in atmospheric PM trace metal content in Spanish towns: Illustrating the chemical complexity of the inorganic urban aerosol cocktail. Atmos. Environ. 40, 6791-6803. https://doi.org/10.1016/j.atmosenv.2006.05.074

Nisbet, I.C.T., LaGoy, P.K., 1992. Toxic equivalency factors (TEFs) for polycyclic aromatic hydrocarbons (PAHs). Regul. Toxicol. Pharm. 16, 290-300. https://doi.org/10.1016/0273-2300(92)90009-X

Ojebuoboh, F., 1992. Bismuth - Production, properties, and applications. JOM 44, 46–49. https://doi.org/10.1007/BF03222821

Pankow, J.F., 1994a. An absorption model of gas/particle partitioning of organic compounds in the atmosphere. Atmos. Environ. 28, 185-188. https://doi.org/10.1016/1352-2310(94)90093-0

Pankow, J.F., 1994b. An absorption model of the gas/aerosol partitioning involved in the formation of secondary organic aerosol. Atmos. Environ. 28, 189-193. https://doi.org/10.1016/1352-2310(94)90094-9

Park, M., Joo, H.S., Lee, K., Jang, M., Kim, S.D., Kim, I., Borlaza, L.J.S., Lim, H., Shin, H., Chung, K.H., Choi, Y.H., Park, S.G., Bae, M.S., Lee, J., Song, H., Park, K., 2018. Differential toxicities of fine particulate matters from various sources. Sci. Rep. 8, 17007. https://doi.org/10.1038/s41598-018-35398-0

Penkała, M., Ogrodnik, P., Rogula-Kozłowska, W., 2018. Particulate matter from the road surface abrasion as a problem of non-exhaust emission control. Environ. 5, 1-13. https://doi.org/10.3390/environments5010009

Pio, C., Cerqueira, M., Harrison, R.M., Nunes, T., Mirante, F., Alves, C., Oliveira, C., Sanchez de la Campa, A., Artiñano, B., Matos, M., 2011. OC/EC ratio observations in Europe: Re-thinking the approach for apportionment between primary and secondary organic carbon. Atmos. Environ. 45, 6121-6132. https://doi.org/10.1016/j.atmosenv.2011.08.045

Piscitello, A., Bianco, C., Casasso, A., Sethi, R., 2021. Non-exhaust traffic emissions: Sources, characterization, and mitigation measures. Sci. Total Environ. 766, 144440. https://doi.org/10.1016/j.scitotenv.2020.144440

Pun, B.K., Seigneur, C., Grosjean, D., Saxena, P., Gas-phase formation of water-soluble organic compounds in the atmosphere: A retrosynthetic analysis. J. Atmos. Chem. 35, 199-223. https://doi.org/10.1023/A:1006261217691

Querol, X., Alastuey, A., Rodríguez, S., Plana, F., Ruiz, C.R., Cots, N., Massagué, G., Puig, O., 2001. PM_{10} and $PM_{2.5}$ source apportionment in the Barcelona Metropolitan Area, Catalonia, Spain. Atmos. Environ. 35, 6407-6419. https://doi.org/10.1016/S1352-2310(01)00361-2

Querol, X., Alastuey, A., Viana, M.M., Rodriguez, S., Artiñano, B., Salvador, P., Garcia do Santos, S., Fernandez Patier, R., Ruiz, C.R., de la Rosa, J., Sanchez de la Campa, Menendez, M., Gil, J.I., 2004. Speciation and origin of PM_{10} and $PM_{2.5}$ in Spain. J. Aerosol Sci. 35, 1151-1172. https://doi.org/10.1016/j.jaerosci.2004.04.002

Querol, X., Viana, M., Alastuey, A., Amato, F., Moreno, T., Castillo, S., Pey, J., de la Rosa, J., Sánchez de la Campa, A., Artíñano, B., Salvador, P., García Dos Santos, S., Fernández-Patier, R., Moreno-Grau, S., Negral, L., Minguillón, M.C., Monfort, E., Gil, J.I., Inza, A., Ortega, L.A., Santamaría, J.M., Zabalza, J., 2007. Source origin of trace elements in PM from regional background, urban and industrial sites of Spain. Atmos. Environ. 41, 7219–7231. https://doi.org/10.1016/j.atmosenv.2007.05.022

Robinson, A.L., Donahue, N.M., Rogge, W.F., 2006. Photochemical oxidation and changes in molecular composition of organic aerosol in the regional context. J. Geophys. Res. 111, D03302, https://doi.org/10.1029/2005JD006265

Shalamzari, M.S., Ryabtsova, O., Kahnt, A., Vermeylen, R., Hérent, M.F., Quetin-Leclercq, J., Van der Veken, P., Maenhaut, W., Claeys, M., 2013. Mass spectrometric characterization of organosulfates related to secondary organic aerosol from isoprene. Rapid Commun. Mass Spectrom. 27, 784-794. https://doi.org/10.1002/rcm.6511

Sharma, S., Chandra, M., Kota, S.H., 2020. Health effects associated with $PM_{2.5}$: a systematic review. Curr. Pollut. Rep. 6, 345-367. https://doi.org/10.1007/s40726-020-00155-3

Szmigielski, R., Surratt, J.D., Vermeylen, R., Szmigielska, K., Kroll, J.H., Ng, N.L., Murphy, S.M., Sorooshian, A., Seinfeld, J.H., Claeys, M., 2007. Characterization of 2-methylglyceric acid

oligomers in secondary organic aerosol formed from the photooxidation of isoprene using trimethylsilylation and gas chromatography/ion trap mass spectrometry. J. Mass Spectrom. 42, 101-116. https://doi.org/10.1002/jms.1146

Turner, A., 2019. Cadmium pigments in consumer products and their health risks. Sci. Total Environ. 657, 1409-1418. https://doi.org/10.1016/j.scitotenv.2018.12.096

USEPA, 2013. Users' Guide and Background Technical Document for USEPA Region 9 - Preliminary Remediation Goals (PRG) Table. URL: https://semspub.epa.gov/work/02/103453.pdf (accessed 19/03/2021).

USEPA, 2017. Regional Screening Level (RSL) Summary Table. URL: https://semspub.epa.gov/work/03/2245073.pdf (accessed 19/03/2021).

USEPA. 2019. IRIS Assessments. URL: https://cfpub.epa.gov/ncea/iris2/atoz.cfm (accessed 19/03/2021).

Valotto, G., Rampazzo, G., Visin, F., Gonella, F., Cattaruzza, E., Glisenti, A., Formenton, G., Tieppo, P., 2015. Environmental and traffic-related parameters affecting road dust composition: A multi-technique approach applied to Venice area (Italy). Atmos. Environ. 122, 596-608. https://doi.org/10.1016/j.atmosenv.2015.10.006

Van Den Heuvel, R., Staelens, J., Koppen, G., Schoeters, G., 2018. Toxicity of urban PM_{10} and relation with tracers of biomass burning. Int. J. Environ. Res. Public Health 15, 320. https://doi.org/10.3390/ijerph15020320

Vicente, E.D., Alves, C.A., 2018. An overview of particulate emissions from residential biomass combustion. Atmos. Res. 199, 159-185. https://doi.org/10.1016/j.atmosres.2017.08.027

Vicente, E.D., Vicente, A., Nunes, T., Calvo, A.I., del Blanco-Alegre, C., Oduber, F., Fraile, R., Amato, F., Alves, C., 2019. Household dust: loadings and PM_{10}-bound plasticizers and polycyclic aromatic hydrocarbons. Atmosphere 10, 785. https://doi.org/10.3390/atmos10120785

Wang, J., Li, X., Jiang, N., Zhang, W., Zhang, R., Tang, X., 2015. Long term observations of $PM_{2.5}$-associated PAHs: Comparisons between normal and episode days. Atmos. Environ. 104, 228-236. https://doi.org/10.1016/j.atmosenv.2015.01.026

Wang, Q., Liu, M., Yu, Y., Li, Y., 2016. Characterization and source apportionment of $PM_{2.5}$-bound polycyclic aromatic hydrocarbons from Shanghai city, China. Environ. Pollut. 218, 118-128. https://doi.org/10.1016/j.envpol.2016.08.037

Wedepohl, K.H., 1995. The composition of the continental crust. Geochim. Cosmochim. Acta 59, 1217-1232. https://doi.org/10.1016/0016-7037(95)00038-2

White, S.J., Jamie, I.M., Angove, D.E., 2014. Chemical characterisation of semi-volatile and aerosol compounds from the photooxidation of toluene and NO_x. Atmos. Environ. 83, 237-244. https://doi.org/10.1016/j.atmosenv.2013.11.023

WHO, 2016. Ambient air pollution: a global assessment of exposure and burden of disease. World Health Organization, Geneva, Switzerland. URL: https://apps.who.int/iris/handle/10665/250141 (accessed 18/03/2021).

Wood, E.C., Knighton, W.B., Fortner, EC., Herndon, S.C., Onasch, T.B., Franklin, J.P., Worsnop, D.R., Dallmann, T.R., Gentner, D.R., Goldstein, A.H., Harley, R.A., 2015. Ethylene glycol emissions from on-road vehicles. Environ. Sci. Technol. 49, 3322-3329. https://doi.org/10.1021/acs.est.5b00557

Wu, D., Wang, Z., Chen, J., Kong S., Deng, H., Shao, G., Wu, G., 2014. Polycyclic aromatic hydrocarbons (PAHs) in atmospheric $PM_{2.5}$ and PM_{10} at a coal-based industrial city: Implication for PAH control at industrial agglomeration regions, China. Atmos. Res. 149, 217-229. https://doi.org/10.1016/j.atmosres.2014.06.012

Xie, M., Barsanti, K.C., Hannigan, M.P., Dutton, S.J., Vedal, S., 2013. Positive matrix factorization of $PM_{2.5}$ - eliminating the effects of gas/particle partitioning of semivolatile organic compounds. Atmos. Chem. Phys. 13, 7381-7393. https://doi.org/10.5194/acp-13-7381-2013

Yan, Y., He, Q., Guo, L., Li, H., Zhang, H., Shao, m., Wang, Y., 2017. Source apportionment and toxicity of atmospheric polycyclic aromatic hydrocarbons by PMF: Quantifying the influence of coal usage in Taiyuan, China. Atmos. Res. 193, 50-59. https://doi.org/10.1016/j.atmosres.2017.04.001

Yin, P., Brauer, M., Cohen, A.J., Wang, H., Li, J., Burnett, R.T., Stanaway, J.D., Causey, K., Larson, S., Godwin, W., Frostad, J., Marks, A., Wang, L., Zhou, M., Murray, C.J.L., 2020. The effect of air pollution on deaths, disease burden, and life expectancy across China and its provinces, 1990-2017: an analysis for the Global Burden of Disease Study 2017. Lancet Planet. Health 4, e386-e398. https://doi.org/10.1016/S2542-5196(20)30161-3

Zhang, F., Zhao, J., Chen, J., Xu, Y., Xu, L., 2011. Pollution characteristics of organic and elemental carbon in $PM_{2.5}$ in Xiamen, China. J. Environ. Sci. 23, 1 342-1349. https://doi.org/10.1016/s1001-0742(10)60559-1

Zhang, K., Chai, F., Zheng, Z., Yang, Q., Zhong, X., Fomba, K.W., Zhou, G., 2018. Size distribution and source of heavy metals in particulate matter on the lead and zinc smelting affected area. J. Environ. Sci. 71, 188-196. https://doi.org/10.1016/j.jes.2018.04.018

Zhang, Y., Yang, L., Zhang, X., Li, J., Zhao, T., Gao, Y., Jiang, P., Li, Y., Chen, X., Wang, W., 2019. Characteristics of $PM_{2.5}$-bound PAHs at an urban site and a suburban site in Jinan in North China Plain. Aerosol Air Qual. Res. 19, 871-884. https://doi.org/ 10.4209/aaqr.2018.09.0353

Zhu, J., Hsu, C.Y., Chou, H.C., Chen, M.J., Chen, J.L., Yang, T.T., Wu, Y.S., Chen, Y.C., 2019. $PM_{2.5}$- and PM_{10}-bound polycyclic aromatic hydrocarbons (PAHs) in the residential area near coal-fired power and steelmaking plants of Taichung City, Taiwan: *In vitro*-based health risk and source identification. Sci. Total Environ. 670, 439-447. https://doi.org/10.1016/j.scitotenv.2019.03.198

$PM_{2.5}$ chemical composition and health risks by inhalation near a chemical complex

Célia Alves[1†], Margarita Evtyugina[1], Estela Vicente[1], Ana Vicente[1], Ismael Casotti Rienda[1], Ana Sanchez de la Campa[2], Mário Tomé[3], Iola F. Duarte[4]

[1]Department of Environment, Centre for Environmental and Marine Studies (CESAM), University of Aveiro, 3810-193 Aveiro, Portugal

[2]Associate Unit CSIC-University of Huelva "Atmospheric Pollution", Centre for Research in Sustainable Chemistry - CIQSO, University of Huelva, E21071 Huelva, Spain

[3]PROMETHEUS, School of Technology and Management (ESTG), Polytechnic Institute of Viana do Castelo, 4900-348 Viana do Castelo, Portugal

[4]Department of Chemistry, CICECO - Aveiro Institute of Materials, University of Aveiro, 3810-193 Aveiro, Portugal

SUPLEMENTARY MATERIAL

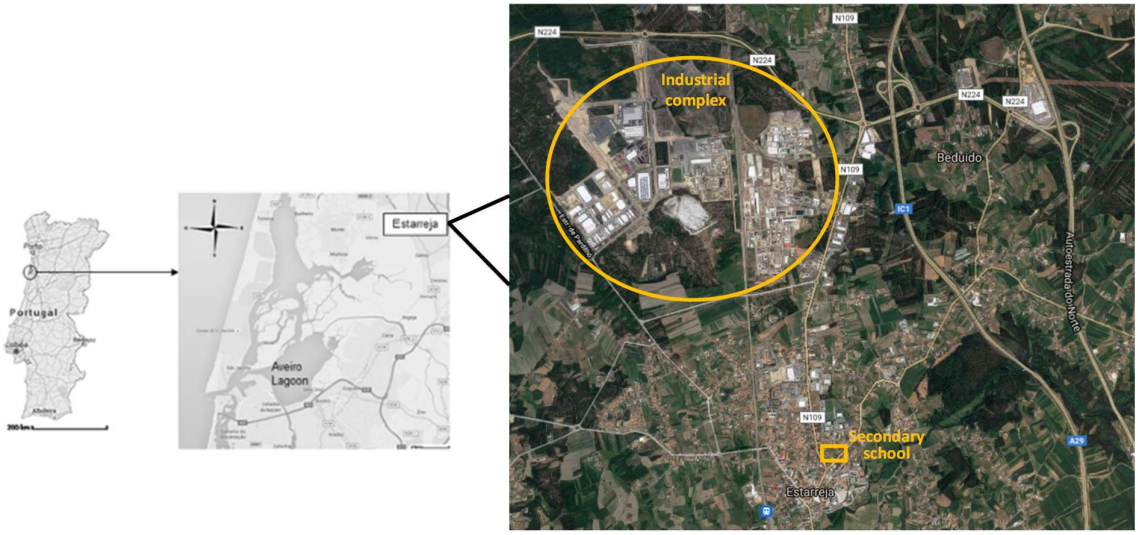

Fig. S1. Location of the sampling site and industrial complex in Estarreja.

† Corresponding author. E-mail: celia.alves@ua.pt

Table S1. Concentrations of oxygenated organic compounds (ng/m^3) in $PM_{2.5}$.

	Minimum	Maximum	Average
n-Alkanols			
1-Decanol	bdl	0.624	0.0500
1-Dodecanol	0.00442	2.12	0.161
1-Tetradecanol	bdl	4.72	0.522
1-Pentadecanol	bdl	1.69	0.354
1-Hexadecanol	0.135	5.24	1.25
1-Octadecanol	0.674	26.0	5.62
1-Docosanol	bdl	5.95	1.22
1-Tricosanol	0.0543	0.836	0.192
1-Tetracosanol	bdl	26.7	5.10
1-Pentacosanol	bdl	12.8	1.04
1-Hexacosanol	bdl	24.6	6.29
1-Heptacosanol	bdl	0.870	0.137
1-Octacosanol	bdl	10.6	1.68
1-Triacontanol	bdl	5.16	0.597
n-Alkanoic and alkenoic acids			
Octanoic acid	0.127	1.58	0.651
Nonanoic acid	0.721	7.10	2.76
Decanoic acid	bdl	1.90	0.529
Undecanoic acid	bdl	0.987	0.265
Dodecanoic acid	0.453	6.61	1.23
Tridecanoic acid	bdl	3.85	0.490
Tetradecanoic acid	1.26	21.9	4.04
Pentadecanoic acid	0.437	5.61	1.09
Hexadecanoic acid	31.9	406	84.9
cis-9-Hexadecenoic acid	bdl	0.964	0.292
Heptadecanoic acid	1.14	12.2	2.51
Octadecanoic acid	48.3	774	158
cis-9-Octadecenoic acid	bdl	8.56	1.30
Nonadecanoic acid	bdl	2.61	0.552
Eicosanoic acid	0.175	22.3	5.17
Heneicosanoic acid	bdl	105	8.54
Docosanoic acid	0.679	28.2	6.35
Tricosanoic	bdl	35.7	6.62
Tetracosanoic acid	bdl	63.1	9.00
Hexacosanoic acid	bdl	13.5	3.46
Octadecanoic acid	bdl	18.1	3.35
Di- and tricarboxylic acids			

Ethanedioic acid (oxalic)	9.56	312	83.1
Butanedioic acid (succinic)	bdl	139	33.8
2-Ethylpropanedioic acid (ethylmalonic)	bdl	46.6	8.67
1,5-Pentanedioic acid (glutaric)	bdl	45.1	9.96
Hydroxybutanedioic acid (malic)	bdl	19.9	3.99
Hexanedioic acid (adipic)	bdl	6.62	2.50
3-Hydroxyhexanedioic acid (3-hydroxyadipic)	bdl	18.2	4.45
Heptanedioic acid (pimelic)	bdl	8.10	1.57
Octanedioic acid (suberic)	bdl	20.8	3.09
Nonanedioic acid (azelaic)	bdl	37.4	10.7
Decanedioic acid (sebacic)	bdl	3.51	0.827
2-Hydroxypropane-1,2,3-tricarboxylic acid (citric)	bdl	12.4	2.61
Hydroxy-, dihydroxy- and oxo-acids			
Glycolic acid (hydroxyethanoic)	bdl	217	46.7
Levulinic acid (4-oxopentanoic)	bdl	26.9	9.62
Hydracrylic acid (3-hydroxypropionic)	0.323	17.2	3.65
3-Hydroxybutyric acid (3-hydroxybutanoic)	bdl	22.2	4.46
4-Deoxyerythronic acid (2,3-dihydroxybutanoic)	6.33	74.2	17.6
Glyceric acid (2,3-Dihydroxypropanoic acid)	0.578	10.4	3.62
Resin acids			
Isopimaric acid	bdl	1.79	0.197
Dehydroabietic acid	bdl	69.1	17.4
Other acids			
γ-Aminobutyric acid (4-aminobutanoic)	bdl	1.58	0.143
2-Furoic acid	bdl	0.941	0.247
Benzoic acid	0.0594	3.05	1.00
Hydroxybenzoic acid	0.171	15.1	3.06
Phthalic acid	bdl	23.5	7.11
Terephthalic acid	1.12	181	54.6
Pinene and isoprene oxidation products			
Pinonic acid	bdl	2.37	0.433
Pinic acid	bdl	57.7	6.61
Pinanediol	bdl	7.72	2.25
2-Methylglyceric acid oligomers	2.09	1697	241
Sterols			
Cholesterol	bdl	1.30	0.167
β-Sitosterol	bdl	4.66	1.08
Glyceridic compounds			
Glycerol	10.3	157	39.6

Monopalmitin	3.97	29.7	14.1
Monostearin	1.95	7.81	4.58
Anhydrosugars and polyols			
Levoglucosan	29.5	1368	302
Mannosan	1.64	197	41.1
Galactosan	0.725	64.5	15.6
Unidentified sugars	9.18	174	62.3
Meso-Erythritol	0.701	30.3	8.53
Quebrachitol	bdl	0.392	0.0901
Phenolic compounds from lignin			
Vanillin	bdl	5.75	1.45
Vanillic acid	bdl	8.25	1.78
Syringic acid	bdl	14.5	3.20
Cinnamic acid	bdl	29.9	2.64
o-Hydroxycinnamic acid (o-coumaric)	1.86	11.4	5.08
p-Hydroxycinnamic acid (p-coumaric)	bdl	10.7	3.45
Glycol compounds			
Ethylene glycol	8.87	92.5	22.6
Diethylene glycol	0.374	35.6	10.2
Triethylene glycol	1.28	11.3	60.9
Tetraethylene glycol	1.24	5.73	3.35
Aromatic ketones			
7,9-Di-tert-butyl-1-oxaspiro[4.5]deca-6,9-diene-2,8-dione	bdl	231	27.6
2,6-Di-tert-butyl-1,4-benzoquinone	10.8	1231	115
Benzoquinone derivative	bdl	110	31.0
Other compounds			
Unidentified phthalates	9.71	90.1	31.5
Hydrocinnamic acid methyl ester	2.93	13.1	7.57
Oxidised Irgafos 168	91.6	1710	327
2,4-Di-tert-butylphenol	bdl	291	51.2

bdl – below detection limit